Universidade de Aveiro Departamento de Química
2017

Sofia Reis Brandão

Caracterização da dinâmica mitocondrial na deficiência múltipla das acil-CoA desidrogenases

Characterization of mitochondrial dynamics in multiple acyl-CoA dehydrogenase deficiency

Universidade de Aveiro Departamento de Química
2017

Sofia Reis Brandão

Caracterização da dinâmica mitocondrial na deficiência múltipla das acil-CoA desidrogenases

Characterization of mitochondrial dynamics in multiple acyl-CoA dehydrogenase deficiency

Dissertação apresentada à Universidade de Aveiro para cumprimento dos requisitos necessários à obtenção do grau de Mestre em Bioquímica, ramo em Bioquímica Clínica, realizada sob a orientação científica da Doutora Rita Maria Pinho Ferreira, professora auxiliar do Departamento de Química da Universidade de Aveiro e do Doutor Hugo Daniel Carvalho de Azevedo Rocha, assistente principal da carreira dos técnicos superiores de Saúde, ramo de Genética no Instituto Nacional de Saúde Doutor Ricardo Jorge do Porto.

Dedico este trabalho à minha família por todo o apoio.

o júri

presidente

Prof. Doutor Francisco Manuel Lemos Amado
Professor Associado com Agregação do Departamento de Química da Universidade de Aveiro

Prof. Doutor António Alexandre Moreira Ribeiro de Ascensão
Professor Auxiliar da Faculdade de Desporto da Universidade do Porto

Prof. Doutor Hugo Daniel Carvalho de Azevedo Rocha
Assistente principal da carreira dos técnicos superiores de Saúde, ramo de Genética no Instituto Nacional de Saúde Doutor Ricardo Jorge do Porto

agradecimentos

Em primeiro lugar quero agradecer à minha orientadora, a Professora Rita Ferreira, por todas as sugestões e correções, pelas oportunidades que me possibilitaram aumentar o conhecimento científico e laboratorial e pelo apoio incansável ao longo deste ano. O empenho e dedicação que demonstra na vida profissional são um exemplo que espero alcançar um dia.

Ao meu co-orientador, o Doutor Hugo Rocha, agradeço pela oportunidade de aprender num ambiente exterior ao da Universidade de Aveiro, no INSA-Porto, e por todos os ensinamentos científicos e laboratoriais. Ter acompanhado o seu trabalho permitiu-me traçar novos objetivos profissionais e pessoais.

Agradeço também às técnicas dos laboratórios que frequentei, Cristina Barros e Lurdes Lopes, pela disponibilidade e paciência que mostraram sempre que lhes pedi ajuda. Um agradecimento especial à Cristina pelas palavras de carinho no final daqueles dias mais difíceis.

Ao José pela companhia no laboratório, sem dúvida conseguiu quebrar a rotina daqueles dias mais monótonos. À Rita Nogueira Ferreira agradeço a enorme paciência e disponibilidade por todos os esclarecimentos e conselhos laboratoriais. À Professora Margarida Fardilha pela facilidade na partilha de informações e receção no iBiMED e claro às suas alunas, a Magda e a Juliana, pelos conhecimentos laboratoriais que me transmitiram e pela simpatia e disponibilidade para colaborar sempre que lhes pedi ajuda.

Aos amigos que me acompanharam nos momentos de desespero e euforia e fizeram com que nunca deixasse de ser quem sou. Carolina, Daniel, Joaquim, Anabela, Gonçalo, Dani, Dinês, Barbara e Inês obrigada por tornarem este ano tão especial e mais fácil. À colega de casa que se tornou numa amiga para a vida, Raquel, obrigada por me fazeres sentir a melhor pessoa do Mundo. As tuas palavras de conforto, mesmo à distância, fizeram a diferença para ignorar os dias difíceis.

Ao meu irmão e aos meus pais agradeço a paciência e carinho que tiveram sempre que fui a casa e não lhes dediquei todo o tempo porque estava ocupada com outras tarefas. Um agradecimento especial à minha mãe pelas longas horas de conversa que passámos ao telemóvel. À restante família agradeço os desafios e amizade com que desde cedo me habituaram, estou certa que me tornaram uma pessoa mais lutadora e persistente.

A todos vós que de uma maneira mais ou menos direta possibilitaram a concretização deste trabalho, o meu mais sincero obrigada.

palavras-chave

β-oxidação de ácidos gordos, rastreio neonatal, dinâmica mitocondrial, proteoma mitocondrial, doenças da β-oxidação mitocondrial de ácidos gordos, deficiência múltipla das acil-CoA desidrogenases.

resumo

As doenças da β-oxidação mitocondrial dos ácidos gordos fazem parte do painel de doenças detetadas no rastreio neonatal na grande maioria dos países desenvolvidos, incluindo Portugal. A deficiência múltipla das acil-CoA desidrogenases é uma das doenças rastreadas, sendo rara e apresentando um padrão de transmissão autossómico recessivo. Esta disfunção no metabolismo dos ácidos gordos é caracterizada por fenótipos bastante distintos, sendo reconhecidas duas formas clínicas: moderada e grave. Estudos anteriores do nosso grupo de investigação revelaram que o proteoma mitocondrial de pacientes homozigotos para a mesma mutação evidencia níveis de expressão diferentes das mesmas proteínas e que os pacientes com formas moderadas da doença apresentam semelhanças e diferenças quando comparados com pacientes com formas graves. O objetivo deste estudo foi relacionar as alterações dos processos biológicos associados à homeostasia mitocondrial com a severidade da doença, associada a mutações no gene que codifica a proteína *electron transfer flavoprotein dehydrogenase* (ETFDH), traçando semelhanças e diferenças.

No geral, o nosso estudo fornece uma perspetiva global da dinâmica mitocondrial nas duas formas da doença. Ambas as formas, moderada e grave, apresentaram biogénese mitocondrial diminuída e adaptação metabólica, suportadas por níveis baixos de *peroxisome proliferator-activated receptor γ coactivator 1 alpha* (PGC-1α) e de gliceraldeído-3-fosfato desidrogenase (GAPDH), respetivamente, em todos os pacientes com a doença. Os níveis de expressão de sirtuina 3 (SIRT3) e a atividade de ATP sintase foram encontrados diminuídos em quase todos os pacientes, sugerindo uma disfunção mitocondrial. Os níveis reduzidos de SIRT3 foram corroborados pela diminuição dos níveis de PGC-1α. Os níveis de expressão das outras proteínas analisadas foram diversos entre os pacientes e, portanto, sugerem que a correlação entre a severidade da doença e as adaptações mitocondriais não é transversal a todas as formas da doença. De facto, os diferentes resultados obtidos podem explicar, pelo menos em parte, a variedade de fenótipos observados em pacientes com a doença. Neste sentido, são necessários mais estudos para compreender melhor a patogénese da doença. No futuro, seria interessante analisar os efeitos da deficiência de ETFDH noutras células em vez de fibroblastos e pesquisar outros metabolitos energéticos relacionados com estes mecanismos.

keywords

Fatty acid β-oxidation, newborn screening, mitochondrial dynamics, mitochondrial proteome, disorders of mitochondrial fatty acid β-oxidation, multiple acyl-CoA dehydrogenase deficiency.

abstract

Mitochondrial fatty acid β-oxidation disorders are some of the many diseases detected by newborn screening in most developed countries, including Portugal. Among screened disorders, multiple acyl-CoA dehydrogenase deficiency (MADD) is a rare autosomal recessively inherited disorder that presents very distinct phenotypes, being recognized in two clinical forms: mild and severe. Previous studies from our research group showed that the mitochondrial proteome of homozygous patients having the same mutation presents different expression levels of the same proteins and that patients with mild forms of MADD share some proteins with severe forms and at the same time present distinctive expression patterns. The aim of this study was to relate the regulation of biological processes associated to mitochondrial homeostasis with the severity of MADD, due to mutations on the gene that codifies the protein electron transfer flavoprotein dehydrogenase (ETFDH), evidencing similarities and differences.

In overall our study provides a global perspective of the mitochondrial dynamics in the two forms of MADD, mild and severe. Both forms presented down-regulation of mitochondrial biogenesis and metabolic adaptation highlighted by lower levels of peroxisome proliferator-activated receptor γ coactivator 1 alpha (PGC-1α) and glyceraldehyde-3-phosphate dehydrogenase (GAPDH), respectively, in all MADD patients. Expression levels of sirtuin 3 (SIRT3) and the activity of ATP synthase were found decreased in almost all patients, suggesting mitochondrial dysfunction. Down-regulation of SIRT3 was corroborated by decreased levels of PGC-1α. The expression levels of the other proteins analyzed were diverse among MADD patients and thus highlighting no straight full correlation between disease severity and mitochondrial adaptations. In fact, the different results obtained may explain, at least in part, the variety of phenotypes observed in MADD patients. So, more studies are needed to better understand MADD pathogenesis. In the future, it would be interesting to analyze the effects of ETFDH deficiency in other cell types rather than fibroblasts and search for other energetic metabolites related with these mechanisms.

Table of contents

Figure Index

Table Index

Abbreviations

ACAD	Acyl-CoA dehydrogenases
Acetyl-CoA	Acetyl-coenzyme A
ACS	Acyl-CoA synthetase
ADP	Adenosine diphosphate
AIF	Apoptosis-inducing factor
AMP	Adenosine monophosphate
AMPK	AMP-activated protein kinase
Apaf-1	Apoptotic protease-activating factor-1
ATG5	Autophagy protein 5
ATP	Adenosine triphosphate
ATPase α	ATP synthase α subunit
Bak	Bcl-2 antagonist killer 1
Bax	Bcl-2 associated X protein
Bcl-2A1	Bcl-2 related protein A1
Bid	BH3-only pro-apoptotic protein
BSA	Bovine serum albumin
C_{5DC}	Glutarylcarnitine
C-I	Nicotinamide adenine dinucleotide-ubiquinone oxidoreductase
C-II	Succinate dehydrogenase
C-III	Ubiquinol-cytochrome c reductase
C-IV	Cytochrome c oxidase
C-V	ATP synthase
CACT	Carnitine/acylcarnitine translocase
cAMP	Cyclic adenosine monophosphate
Casp-	Caspase (cysteine-aspartic protease), number refers to the type of caspase
C_{number}	Acylcarnitine species with the corresponding carbon chain length
$C_{number\text{-}OH}$	3-Hydroxyacylcarnitine species with the corresponding carbon chain length
CoASH	Coenzyme A

CoQ	Ubiquinone (Coenzyme Q10)
COX IV	Subunit IV of cytochrome c oxidase
CPT	Carnitine palmitoyltransferase
CS	Citrate synthase
Cyt c	Cytochrome c
DISC	Death-inducing signaling complex
DMEM	Dulbecco's Modified Eagle Medium
DNA	Deoxyribonucleic acid
DNP	2,4-Dinitrophenyl
DNPH	2,4-Dinitrophenylhydrazine
DR	Death receptors
Drp1	Dynamin-related protein 1
DTNB	5,5'-Dithiobis-(2-nitrobenzoate)
ECH	2-Enoyl-CoA hydratases
EMA	Ethylmalonic acid
EndoG	Endonuclease G
ER	Endoplasmic reticulum
ERRs	Oestrogen-related receptors
ESI	Electrospray ionization
ETF	Electron transfer flavoprotein
ETFDH	ETF dehydrogenase
ETF-QO	ETF-ubiquinone oxidoreductase
FA	Fatty acids
FAD	Flavin adenine dinucleotide
$FADH_2$	Reduced form of FAD
FAO	Mitochondrial fatty acid β-oxidation
FAOD	Mitochondrial fatty acid β-oxidation disorders
FasL	Fas ligand
Fis1	Mitochondrial fission 1 protein
Fzo	*Drosophila* mitofusin gene
GA	Glutaric aciduria
GAPDH	Glyceraldehyde-3-phosphate dehydrogenase

GPx	Glutathione peroxidase
HAD	3-Hydroxyacyl-CoA dehydrogenases
HIF-1α	Hypoxia-inducible factor-1α
IAPs	Inhibitor of apoptosis proteins
INSA	National Institute of Health Doctor Ricardo Jorge
KAT	3-Ketoacyl-CoA thiolases
LACS	Long-chain acyl-CoA synthetase
LCAD	Long-chain acyl-CoA dehydrogenase
LC-carnitine	Long-chain fatty acylcarnitine ester
LC-CoA	Long-chain fatty acyl-CoA ester
LCECH	Long-chain 2-enoyl-CoA hydratase
LCFA	Long-chain fatty acids
LCHAD	Long-chain 3-hydroxyacyl-CoA dehydrogenase
LCKAT	Long-chain 3-ketoacyl-CoA thiolase
MAD	Multiple acyl-CoA dehydrogenase
MADD	Multiple acyl-CoA dehydrogenase deficiency
MAPK	Mitogen-activated protein kinase
MCAD	Medium-chain acyl-CoA dehydrogenase
MCADD	Medium-chain acyl-CoA dehydrogenase deficiency
MC-CoA	Medium-chain fatty acyl-CoA ester
MCFA	Medium-chain fatty acids
MCKAT	Medium-chain 3-ketoacyl-CoA thiolase
Mfns	Mitofusins
MnSOD	Manganese superoxide dismutase
mRNA	Messenger ribonucleic acid
M/SCHAD	Medium/Short-chain 3-hydroxyacyl-CoA dehydrogenase
MS/MS	Tandem mass spectrometry
mtDNA	Mitochondrial DNA
mtGSH	Mitochondrial glutathione
MTP	Mitochondrial trifunctional protein
MTP18	Mitochondrial membrane protein 18
mtTFA	Mitochondrial transcription factor A

NAD^+	Nicotinamide adenine dinucleotide
NADH	Reduced form of NAD^+
NBS	Newborn screening
NC	Negative control
NMD	Nonsense-mediated mRNA decay
NR	Not reported
NRFs	Nuclear respiratory factors
OD	Optical density
Omi/HtrA2	High-temperature requirement A2 serine protease
OPA1	Mitochondrial dynamin-like 120 kDa protein
OXPHOS	Oxidative phosphorylation
PBS	Phosphate-buffered saline
PGC-1	Peroxisome proliferator-activated receptor γ coactivator 1
Pi	Inorganic phosphate
PKA	Protein kinase A
PPAR	Peroxisome proliferator-activated receptor
PQC	Protein quality control
Prx III	Peroxiredoxin mitochondrial
PTP	Permeability transition pore
ROS	Reactive oxygen species
RNS	Reactive nitrogen species
RR-MADD	Riboflavin-responsive MADD
SCAD	Short-chain acyl-CoA dehydrogenase
SC-CoA	Short-chain fatty acyl-CoA ester
SCECH	Short-chain 2-enoyl-CoA hydratase
SCFA	Short-chain fatty acids
SCHAD	Short-chain 3-hydroxyacyl-CoA dehydrogenase
SD	Standard deviation
SDS	Sodium dodecyl sulphate
SDS-PAGE	SDS-polyacrylamide gel electrophoresis
SIRT	Sirtuin (silent information regulator two (Sir2) protein)
Smac/Diablo	Second mitochondria-derived activator of caspase/direct IAP binding

	protein with low isoelectric point
TBS	Tris-buffered saline
TG	Triacylglycerides
TNB	2-Nitro-5-thiolbenzoate
TNF	Tumor necrosis factor
TRAIL	TNF-related apoptosis-inducing ligand
Trx II	Thioredoxine mitochondrial
TTBS	TBS with Tween 20
UCP2	Uncoupling protein 2
VLCAD	Very long-chain acyl-CoA dehydrogenase
VLCADD	Very long-chain acyl-CoA dehydrogenase deficiency

1. Introduction

Fatty acid oxidation defects are a group of inherited metabolic disorders, affecting the enzymes involved in the oxidation of fatty acids (1,2). These disorders are usually transmitted in an autosomal recessive pattern being individually rare, but together they represent a large and important group of inherited metabolic disorders (1). Patients have heterogeneous clinical phenotypes and the same metabolic blockage may be associated to very different clinical phenotypes. The main affected organs include heart, liver and skeletal muscles (2). The mortality and morbidity rates associated with these conditions can be prevented, or at least decreased, if disorders are early recognized and treated (1). Indeed, fatty acid oxidation disorders can lead to serious health problems and even to death if not treated or when the diagnosis is done too late. The advantages of an early intervention make this group of disorders main targets of newborn screening (NBS) programs worldwide (1,3,4). The NBS aims to identify newborns with serious but treatable health diseases before the onset of symptoms and the development of irreversible damage (5,6). Since the introduction of tandem mass spectrometry (MS/MS) into screening programs in the 1990s, the number of inherited metabolic disorders screened greatly increased, including amino acid, organic acid and fatty acid metabolism disorders, since this technique allows the simultaneously determination of many analytes on the same analysis (1,5). NBS is one of the most successful public health programs initiated in the last fifty years (1,6).

Among mitochondrial fatty acid β-oxidation (FAO) disorders, multiple acyl-CoA dehydrogenase deficiency (MADD) is one of the twenty-five disorders screened by NBS in Portugal. The birth prevalence of MADD is 1:164,765 in Portugal (7). These FAO disorders (FAOD) result from defects in enzymes of mitochondrial fatty acid β-oxidation; however, in most cases the association between the phenotype and the genotype is not straightforward (2,8), which suggest that other individual cellular/molecular mechanisms might interfere with disease pathogenesis. Herein, we overview FAO metabolism, its regulation and contextualize MADD, the chosen model to study mitochondrial dynamics disturbances in FAO. We also critically analyze the potential contribution of the molecular pathways harbored in mitochondria or involved in the regulation of its functionality to the pathogenesis of FAOD, giving emphasis to MADD.

1.1. Mitochondrial fatty acid β-oxidation

The main function of mitochondrial fatty acid β-oxidation (FAO) is to generate acetyl-coenzyme A (acetyl-CoA) and reducing equivalents such as flavin adenine dinucleotide ($FADH_2$) and nicotinamide adenine dinucleotide (NADH), especially during periods of fasting and metabolic stress. These molecules are linked to the Krebs cycle and to the oxidative phosphorylation (OXPHOS) system leading to energy production in the form of adenosine triphosphate (ATP) (9,10). Figure 1 overviews the FAO pathway from the activation of fatty acids to the generation of acetyl-CoA and its association with the Krebs cycle and OXPHOS.

OXPHOS is the key metabolic pathway in mitochondrial energy production. It requires the action of five multiheteromeric complexes located in the inner mitochondrial membrane, designated complexes I to V (11,12). Electrons donated from NADH are passed from complex I to complex III through ubiquinone (CoQ). In addition, CoQ also takes electrons from succinate via complex II and from electron transfer flavoprotein-ubiquinone oxidoreductase (ETF-QO). Finally, cytochrome c (Cyt c), an iron-containing heme protein, shuttles electrons from complex III to IV, which transfers its electrons to oxygen (O_2), the final electron acceptor. During this process, the electrochemical gradient generated by the pumping of protons out of the mitochondrial inner membrane to the intermembrane space, is used by complex V in order to convert adenosine diphosphate (ADP) to ATP (12) (Figure 1).

Adipose tissue triacylglycerides (TG) are the primary source of fatty acids (FA) used for FAO. During fasting conditions TG are mobilized, transported and distributed to various tissues through bloodstream in lipoproteins (9). Once inside the cells, long-chain FA (LCFA) are activated to their coenzyme A (CoASH) esters and transported into mitochondria for subsequent β-oxidation (9,10,13). The transporter involved in the process corresponds to the “carnitine shuttle” that requires the concerted action of three proteins: carnitine palmitoyltransferase 1 (CPT1), carnitine/acylcarnitine translocase (CACT), and carnitine palmitoyltransferase 2 (CPT2). CPT1 converts acyl-CoA compounds to their acylcarnitine metabolites at the outer mitochondrial membrane. CACT transports the acylcarnitines across the inner mitochondrial membrane in exchange for free carnitine, and CPT2 re-esterifies the acylcarnitines to their acyl-CoA esters on the inner mitochondrial membrane (13). In contrast, the short-chain and medium-chain FA (SCFA and MCFA)

diffuse freely across the mitochondrial membrane into the matrix, where they are activated to their corresponding acyl-CoA esters, which are oxidized by FAO enzymes (9,10,14). Once in the mitochondrial matrix FA are oxidized by the β-oxidation system (Figure 1).

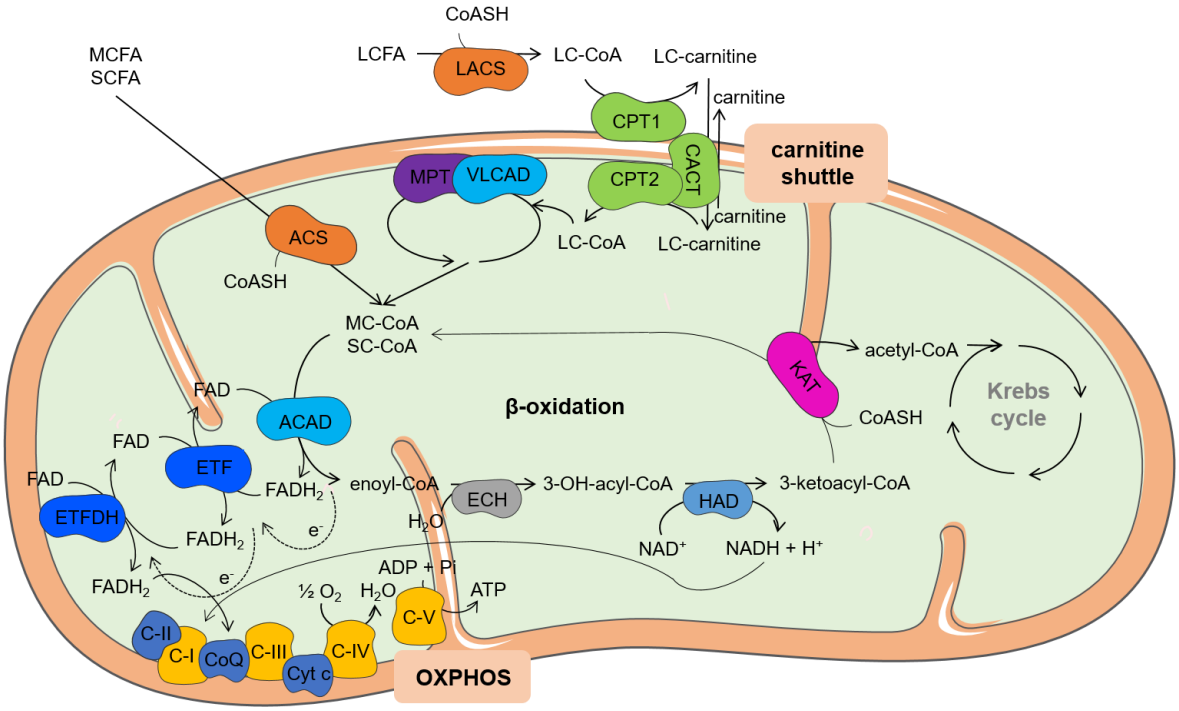

Figure 1. Schematic representation of mitochondrial fatty acid β-oxidation and its association with Krebs cycle and OXPHOS. Figure made with *Servier Medical Art*. Abbreviations: ACAD: acyl-CoA dehydrogenases, acetyl-CoA: acetyl-coenzyme A, ACS: acyl-CoA synthetase, ADP: adenosine diphosphate, ATP: adenosine triphosphate, C-I: nicotinamide adenine dinucleotide-ubiquinone oxidoreductase, C-II: succinate dehydrogenase, C-III: ubiquinol-cytochrome c reductase, C-IV: cytochrome c oxidase, C-V: ATP synthase, CACT: carnitine/acylcarnitine translocase, CoASH: coenzyme A, CoQ: ubiquinone, CPT1: carnitine palmitoyltransferase 1, CPT2: carnitine palmitoyltransferase 2, Cyt c: cytochrome c, e^-: electrons, ECH: 2-enoyl-CoA hydratases, ETF: electron transfer flavoprotein, ETFDH: electron transfer flavoprotein dehydrogenase, FAD: flavin adenine dinucleotide, $FADH_2$: reduced form of FAD, HAD: 3-hydroxyacyl-CoA dehydrogenases, H_2O: water, KAT: 3-ketoacyl-CoA thiolases, LACS: long-chain acyl-CoA synthetase, LC-carnitine: long-chain fatty acylcarnitine ester, LC-CoA: long-chain fatty acyl-CoA ester, LCFA: long-chain fatty acids, MC-CoA: medium-chain fatty acyl-CoA ester, MCFA: medium-chain fatty acids, MTP: mitochondrial trifunctional protein, NAD^+: nicotinamide adenine dinucleotide, NADH: reduced form of NAD^+, O_2: oxygen, OH: hydroxy, OXPHOS: oxidative phosphorylation, Pi: inorganic phosphate, SC-CoA: short-chain fatty acyl-CoA ester, SCFA: short-chain fatty acids, VLCAD: very long-chain acyl-CoA dehydrogenase.

The β-oxidation cycle is characterized by four sequential steps in which an acyl-CoA ester undergoes dehydrogenation, hydration, dehydrogenation again and finally thiolytic cleavage (Figure 1). These steps are catalyzed by enzymes with overlapping chain length specificities (10,14). Beta-oxidation can also occur in peroxisomes, although it is different from mitochondrial oxidation in terms of enzymology, regulation, energy production and especially substrate specificity (15,16). Indeed, LCFA are mainly oxidized in peroxisomes and after shortening of their chain length, they are transported to mitochondria (15). Inside mitochondria, FA are metabolized by FAO enzymes and fully oxidized to carbon dioxide (CO_2) and water (H_2O) by Krebs cycle and OXPHOS, respectively (14). There are another types of FA oxidation such as α- and ω-oxidation, which require additional enzymes for the oxidation of branched-chain or odd-numbered FA (14,17).

The first step in β-oxidation cycle is catalyzed by at least three distinct acyl-CoA dehydrogenases (ACAD), each having preference for acyl-CoA substrates of differing chain lengths: very long-chain acyl-CoA dehydrogenase (VLCAD) acts on C_{12}-C_{24} substrates, medium-chain acyl-CoA dehydrogenase (MCAD) acts on C_6-C_{16} substrates, and short-chain acyl-CoA dehydrogenase (SCAD) acts on C_4-C_6 substrates (14,18). There are other two additional ACAD with less well established physiological roles: long-chain acyl-CoA dehydrogenase (LCAD) and acyl-CoA dehydrogenase 9 (19). SCAD, MCAD and LCAD are soluble, mitochondrial matrix enzymes composed of four identical subunits with a native molecular mass of 160-180 kDa, whereas VLCAD is membrane-bound and is not a tetramer but a dimer of two identical subunits of about 70 kDa. Each of these subunits carries a flavin adenine dinucleotide (FAD) noncovalently bound at the active site, supporting the activity of these enzymes in the catalysis of a FAD-linked dehydrogenation (18). Reoxidation of the reduced flavoproteins is possible by electron transfer flavoprotein (ETF), which has FAD as prosthetic group, and passes reducing equivalents to another flavoprotein called electron transfer flavoprotein-ubiquinone oxidoreductase (ETF-QO) (18,20). ETF-QO, also designated as electron transfer flavoprotein dehydrogenase (ETFDH), passes its electrons to the mitochondrial electron transport chain via CoQ (Figure 1). ETF is a dimer of two nonidentical subunits, α and β, containing one FAD molecule and is localized in the mitochondrial matrix, while ETFDH is a flavoprotein localized in the inner mitochondrial membrane with 68 kDa (9,20). Crystallographic studies support the association ACAD-ETF-ETFDH during electron and

hydrogen transfer from ETFDH to CoQ, which delivers electrons to complex III of OXPHOS (20) (Figure 1).

The second step of β-oxidation is the hydration of 2-trans-enoyl-CoAs to their corresponding 3-hydroxyacyl-CoAs catalyzed by 2-enoyl-CoA hydratases (ECH) (Figure 1). There are at least two distinct enzymes: crotonase and long-chain 2-enoyl-CoA hydratase (LCECH). The first, composed of six identical subunits, is most active for short-chain substrates, while the second, responsible for hydration of long-chain substrates, is part of the mitochondrial trifunctional protein (MTP) (10,14).

The third step of the β-oxidation cycle involves the dehydrogenation of 3-hydroxyacyl-CoAs to 3-oxoacyl-CoAs by two distinct forms of 3-hydroxyacyl-CoA dehydrogenases (HAD) (Figure 1). Short- and medium-chain substrates are preferentially dehydrogenated by a generic short- to medium-chain hydroxyacyl-CoA dehydrogenase, which was first described as short-chain 3-hydroxyacyl-CoA dehydrogenase (SCHAD), a dimer of two identical subunits of 33 kDa each. Long-chain 3-hydroxyacyl-CoA dehydrogenase (LCHAD) is the other specific enzyme and belongs to the MTP (9,14).

In the last step of β-oxidation, 3-ketoacyl-CoAs are converted to acetyl-CoA and its corresponding acyl-CoA ester two-carbon atoms shorter by thiolytic cleavage (9,10) (Figure 1). This reaction is catalyzed by thiolases, which exist in three different isoforms. One thiolase, a homotetramer of 42 kDa subunits localized in the mitochondrial matrix, is specific for acetoacetyl-CoA and 2-methylacetoacetyl-CoA. The other thiolase, often called general thiolase or medium-chain 3-ketoacyl-CoA thiolase (MCKAT), acts on substrates ranging from C_4 to C_{12}. The third thiolase is the long-chain specific thiolase and is one of three proteins of the MTP. MTP is a heterooctamer with four α- and four β-subunits. The α-subunit carries the enzymes of the second and third steps of β-oxidation cycle (LCECH and LCHAD), whereas the β-subunit harbors the thiolase component (9,10,14).

In overall, there are at least twenty-five enzymes and specific transport proteins involved in FAO and defects in many of them are associated with human diseases (2,4,21,22).

1.2. Disorders of mitochondrial fatty acid β-oxidation

Several diseases related to defects in β-oxidation enzymes have been identified, which are generally designated as mitochondrial fatty acid β-oxidation disorders (FAOD) (2,23). FAOD are generally inherited in an autosomal recessive pattern and are individually rare, although they are collectively common (1,2). The inherited metabolic defects can be assigned to two groups: (a) those associated with the "carnitine shuttle", for example CPT1; and (b) those of β-oxidation spiral, such as SCAD, ETF and ETFDH (23). In table 1 are represented FAOD from the two distinct groups mentioned above, their protein, gene and locus defect, the main acylcarnitines found in plasma and the year which they were first described.

Most FAOD are identified by the acylcarnitine profile analyzed by flow injection electrospray ionization (ESI) tandem mass spectrometry (MS/MS) (3,24). In fact, the acylcarnitine profile data obtained from NBS programs is crucial for the diagnosis of FAOD and consequently to estimate its birth prevalence (4). The birth prevalence is a more robust evidence of FAOD since there are significant cases of patients that only present symptoms in late infancy or adulthood. In Portugal, the overall birth prevalence of FAOD is 1:5,991 live births (7). The acylcarnitine profile found in patients with CPT1 and CPT2/CACT deficiencies is very distinct from those observed for ETF and ETFDH deficiencies (Table 1). The CPT1 deficiency is associated with elevated levels of free carnitine (C_0) in plasma and absence of long-chain acylcarnitines due to its inability to produce these metabolites (2). In opposite, patients with CPT2/CACT deficiencies present elevated levels of long-chain acylcarnitines (C_{16}, $C_{16:1}$, C_{18}, $C_{18:1}$) since they are formed but are not correctly transported through the mitochondrial membrane. Deficiencies in ETF and ETFDH proteins are associated with a varied acylcarnitine profile, ranging from short-chain (C_4) to long-chain (C_{14}, C_{16}) acylcarnitines, since they compromise the function of the different chain-specific acyl-CoA dehydrogenases (1,23). However, when the defect is in a specific acyl-CoA dehydrogenase (SCAD or VLCAD deficiency) the acylcarnitine profile observed is representative of its chain specific substrates (Table 1).

Table 1. Genetic and biochemical characteristics of the mitochondrial fatty acid β-oxidation disorders. Gene, locus and year information was collected from Sim *et al.* (23) and Gregersen *et al.* (28) while the information for acylcarnitine profiles was adapted from Sahai *et al.* (1) and Sim *et al.* (23). Acylcarnitine profile was further completed with information from Olsen *et al.* (8).

Deficiency	**Protein**	**Gene**	**Locus**	**Acylcarnitine profiles**	**Year[a]**
Carnitine shuttle					
Carnitine/acylcarnitine translocase	CACT	*SLC25A2*	3p21	C_{16}, $C_{16:1}$, C_{18}, $C_{18:1}$	1992
Carnitine palmitoyltransferase 1 (liver)	CPT1A	*CPT1A*	11q13	C_0	1981
Carnitine palmitoyltransferase 2	CPT2	*CPT2*	1p32	C_{16}, $C_{16:1}$, C_{18}, $C_{18:1}$	1973
β-oxidation spiral					
Electron transfer flavoprotein-α	ETFα	*ETFA*	15q23	C_4, C_5, C_{5DC}, C_6, C_8, C_{10}, C_{12}, C_{14}; $C_{5\text{-}OH}$, $C_{14:1}$, C_{16}, $C_{16:1}$	1986
Electron transfer flavoprotein-β	ETFβ	*ETFB*	19q13		1991
Electron transfer flavoprotein dehydrogenase	ETFDH	*ETFDH*	4q32		1985
Long-chain 3-hydoxyacyl-CoA dehydrogenase (isolated)	LCHAD	*HADHA*	2p23	$C_{14\text{-}OH}$, $C_{16\text{-}OH}$, $C_{18\text{-}OH}$, $C_{18:1\text{-}OH}$	1988
Long-chain 3-ketoacyl-CoA thiolase	LCKAT	*HADHB*	2p23	$C_{16\text{-}OH}$, $C_{18\text{-}OH}$, $C_{18:1\text{-}OH}$	1996
Medium-chain acyl-CoA dehydrogenase	MCAD	*MCAD*	1p31	C_6, C_8, C_{10}, $C_{10:1}$	1982
Medium-chain 3-ketoacyl-CoA thiolase	MCKAT	*ACAA2*	NR	C_4 to C_8	1997
Medium/Short-chain 3-hydroxyacyl-CoA dehydrogenase	M/SCHAD	*HADHSC*	4q22-26	$C_{4\text{-}OH}$, $C_{6\text{-}OH}$, $C_{8\text{-}OH}$	1996
Mitochondrial trifunctional protein-α	LCECH LCHAD	*HADHA*	2p23	$C_{16\text{-}OH}$, $C_{18\text{-}OH}$, $C_{18:1\text{-}OH}$	1992
Mitochondrial trifunctional protein-β	LCKAT	*HADHB*	2p23		
Short-chain acyl-CoA dehydrogenase	SCAD	*ACADS*	12q22	C_4	1984
Very long-chain acyl-CoA dehydrogenase	VLCAD	*ACADVL*	17p11	C_{14}, $C_{14:1}$, $C_{14:2}$, C_{16}, $C_{18:1}$	1993

a: Year of the first defect described. Abbreviations: C_{5DC}: glutarylcarnitine, C_{number}: acylcarnitine species with the corresponding carbon chain length, $C_{number\text{-}OH}$: 3-hydroxyacylcarnitine species with the corresponding carbon chain length, NR: not reported.

The symptoms of FAOD are diverse according to the type of defective enzyme being associated with reduced production of energy-yielding substrates (acetyl-CoA and ketone bodies) and accumulation of free fatty acids and toxic acyl-CoA intermediates and their respective acylcarnitines and acylglycines in tissues (2,22,25). The main organs affected are skeletal muscle, heart and liver since they are highly reliable on FAO to obtain energy. Consequently, the principal symptoms include fasting hypoglycemia, rhabdomyolysis, cardiomyopathy or hepatic dysfunction (2,22). However, hypoketotic hypoglycemia is the hallmark, being present in almost all disorders due to shortage of acetyl-CoA and ATP which lead to sustain glucose and ketone bodies formation (2,21,22,25). In general, acute symptoms are precipitated by infections, fasting, prolonged exercise and stress because these conditions require energy from FAO metabolism resulting in increased levels of accumulated metabolites (2,25).

Some FAOD, including CPT2 deficiency, VLCAD deficiency (VLCADD) and multiple acyl-CoA dehydrogenase deficiency (MADD), have showed a certain degree of correlation between genotype and phenotype, whereas for MCAD deficiency (MCADD), which is the most incident FAOD in Portugal with a birth prevalence of 1:7,973 (7), the phenotype-phenotype correlation is poor (26–28). In fact, the clinical heterogeneous phenotypes observed in FAOD result from the interaction among the genetic mutations, their interactions with other genes and with environmental factors. Consequently, understand the molecular mechanisms underlying these interactions is crucial to better elucidate the pathophysiology of FAOD (27,28).

1.2.1. Multiple acyl-CoA dehydrogenase deficiency

Multiple acyl-CoA dehydrogenase deficiency (MADD) is a rare disorder of fatty acid, amino acid and choline metabolism inherited in an autosomal recessive pattern (29,30). The clinical signs observed are due to defects in electron transfer flavoprotein (ETF) or electron transfer flavoprotein dehydrogenase (ETFDH) proteins, which leads to secondary defects of FAD-dependent enzymes such as acyl-CoA dehydrogenases (29,31). These two proteins, ETF and ETFDH, are essential factors for the flavoproteins to deliver electrons to ubiquinone (CoQ) and therefore they make the interplay between β-oxidation and OXPHOS. The recommended long-term treatment of MADD includes riboflavin, carnitine or glycine, and a diet restricted in fat and protein and high in carbohydrate. In addition to these, fasting avoidance is also recommended (32,33).

In Portugal, the prevalence of MADD is 1:164,765 according to the report of the Portuguese Newborn Screening Program (7). MADD was firstly described in 1976 by Przyrembel and co-workers (34). The main findings retrieved from patient's analysis were the excretion of glutarate, isovalerate, severe untreatable hypoglycemia, elevation of long-chain fatty acids in serum and fatty infiltration of the liver. These evidences do not correlate to those described in the cases of glutaric aciduria type I (GA I) (35,36); however, as the main biochemical abnormality was the excess of glutaric acid, the authors proposed the designation of glutaric aciduria type II (GA II). This denomination distinguishes it from GA I, which is due to isolated glutaryl-CoA dehydrogenase deficiency (35,36). Actually the term MADD is more used because it describes more precisely the metabolic deficiency, although GAII is still used (37).

MADD is generally characterized by hypoketotic hypoglycemia and by accumulation and excretion of abnormal amounts of organic acids derived from the substrates of acyl-CoA dehydrogenases (1,23,29). In addition to the acylcarnitine profile reported by Sahai e*t al.*(1) and Sim *et al.* (23), MADD is also characterized by elevated concentrations of C_{16}, $C_{16:1}$, $C_{14:1}$, $C_{5\text{-}OH}$, and ethylmalonic acid (EMA) (8) (Table 1). This acylcarnitine pattern, ranging from short- to long-chain, support that almost all acyl-CoA dehydrogenases are malfunctional. ETF is a dimer of two nonidentical subunits, α and β, derived from *ETFA* (locus 15q23) and *ETFB* (locus 19q13) genes, respectively. ETFDH is codified by locus 4q32 from *ETFDH* gene (23) (Table 1). Thus, mutations on *ETFA*, *ETFB* and *ETFDH* genes decrease the *in vivo* activity for all the acyl-CoA dehydrogenases. Indeed, the

ETF/ETFDH complex is essential for the acyl-CoA dehydrogenases functionality since it accept electrons and protons and transfer them to CoQ (31,37,38). The polymorphism α-T171, which is responsible for a significant decrease of thermal stability in the *ETFA* gene was reported as significantly overrepresented in VLCADD patients with mild childhood presentation (38). Therefore, the residual levels of VLCAD enzyme activity observed in these patients support the importance of the ETF/ETFDH proteins in FAO metabolism and consequently gives evidence of protein-protein interactions as a possible mechanism underlying the pathophysiology of FAOD.

1.2.1.1. Relation between genotype and phenotype in MADD

Patients with MADD have been classified in three distinct clinical forms (22,33,39). In the neonatal-onset form (type I), the patients are often premature and characterized by dysmorphic features including high forehead, hypoplastic midface, wide-open anterior fontanel, abnormal genitalia and renal cysts. In addition, they can present hypotonia, hepatomegaly, hypoketotic hypoglycemia, metabolic acidosis and excretion of large amounts of abnormal fatty acid and organic acid metabolites (22). Generally, most of these patients die within the first week of life. In type II, the clinical presentation is most likely type I, but without the congenital abnormalities (39). The patients' phenotype of mild- or late-onset forms (type III) is extremely variable, ranging from recurrent episodes of lethargy, vomiting, hypoglycemia, metabolic acidosis and hepatomegaly often triggered by fever, infection or fasting to progressive lipid storage myopathy in adulthood or even asymptomatic cases (22,33,39).

Riboflavin-responsive multiple acyl-CoA dehydrogenase deficiency (RR-MADD) is a variant of MAD defects, firstly described in 1982 (40). In the originally studied patient, the urine organic acid and plasma acylcarnitine profile were abnormal and similar to those with other forms of multiple acyl-CoA dehydrogenation defects, and normalized after riboflavin treatment (40). Riboflavin is the precursor of FAD, which is a cofactor for many enzymes such as acyl-CoA dehydrogenases, ETFDH and other mitochondrial enzymes, acting as a chaperone too, being essential for the folding and stability of these flavoproteins (8,41). All the patients with RR-MADD studied by Olsen and co-workers

(42) harbored pathogenic variations in the *ETFDH* gene. These variations may affect the biogenesis, stability and activity of the ETFDH protein (42). Indeed, patients with RR-MADD showed milder folding defects of ETFDH variants, with a significant increase in protein stability and activity after riboflavin treatment (43). It is not clear whether lack of ETFDH or aberrant accumulated ETFDH protein affects FAD functionality or its precursors (42,44). When mutations in *ETFDH*, *ETFA* or *ETFB* genes are not present, the possibility of defects on riboflavin transporters should be investigated. In fact, these defects lead to cellular riboflavin deficiency, which biochemical and clinical abnormalities may mimic MADD and is possible that some patients with genetic riboflavin transporter defects have been misdiagnosed with MADD (33,41,45). Since the pathogenic variations are generated by single nucleotide substitutions and localized near the CoQ or FAD binding domains, patients suspected of RR-MAD should be treated with both riboflavin and CoQ (37).

For the three clinical types of MADD it has been described a certain degree of correlation between genotype and phenotype (26,46). Indeed, nonsense, frameshift and splice junction mutations that may lead to messenger ribonucleic acid (mRNA) degradation by the nonsense-mediated mRNA decay (NMD) system or by other processes result in complete absence of functional protein are associated with severe, in many cases fatal, clinical disease (severe MADD). On opposition, missense mutations and small in-frame deletions and insertions are usually associated with milder clinical presentations (mild MADD) (37,47). Commonly, homozygosity for null *ETF* or *ETFDH* mutations is associated with the type I/II (26,39). The late-onset patients carry at least one missense variation, especially in *ETFDH* gene, while *ETFA* or *ETFB* mutations are less common in these individuals. Interestingly, almost patients with late-onset MADD are clearly responsive to riboflavin, since they usually present a *ETFDH* missense mutation which is more common associated with RR-MADD phenotypes (33). In table 2 are presented the number of these mutations type for each gene associated with MADD.

Table 2. Type and number of gene mutations in MADD. Adapted from Gregersen *et al.* (47).

Gene	Splice changes	Stop codons	Out-of-frame deletion/insertions	In-frame deletion/insertions	Missense variations
ETFA	1	2	5	1	11
ETFB	2			1	5
ETFDH	2	3	6		17

Indeed, a higher number of missense variations has been identified in *ETFDH* gene compared to the other genes (Table 2). According to this, it would be expected milder phenotypes related to *ETFDH* mutations. However, severe forms for this gene have been reported (48,49). The genotype-phenotype correlation in MADD is poor due to other factors that may modulate the clinical phenotype. Exogenous factors such as febrile infections, cellular temperature, a restricted diet and other physiologic stressors, in addition of the disease-causing mutation, contribute to heterogeneous phenotypes (26,33).

ETF deficiency, due to changes of one of its subunits, results in substrate blockage, and depending on the nature of the causing mutations may lead to the accumulation of misfolded, inactive conformations of ETF proteins (26). The mitochondrial functionality is consequently disturbed, resulting in energy deficiency, accumulation of hydrogens and reducing equivalents, increase in ROS production and oxidative stress (46). When monomeric ETFDH is missing or present but defective, the effects are similar to those in the ETF deficiency (26). So, deficiencies in both ETF and ETFDH lead to the accumulation and excretion of metabolites that reflect functional deficiency of ETF/ETFDH-dependent enzymes, damaging and inactivating them, disabling the shuttle of reducing equivalents and resulting in increased ROS (37,42).

Interestingly, the increase of ROS levels, produced directly by electron leakage from misfolding variant ETFDH proteins or as result of mitochondrial dysfunction, triggers activation of cellular defense signaling pathways to facilitate cellular adaption to mutation (50). It was reported that mild misfolding of ETFDH enzymes, with impaired CoQ binding, results in increased content of superoxide radical anion ($O_2^{\bullet -}$), due to the disturbed electron transfer pathway from the ETFDH to CoQ. (43). Indeed, several studies associate these biochemical alterations with increased oxidative stress (26,42,43,46,48). Therefore, the subjacent mechanisms that regulate cell homeostasis and signaling pathways are

dysregulated, leading to multi-organ failure and the observed clinical phenotypes (50). Thus, the study of the molecular pathways harbored in mitochondria or involved in the regulation of its functionally is crucial to understand the pathogenesis of MADD and therefore in FAOD, since mitochondrial dysfunction have been related with these disorders (27,46,51).

1.3. The role of mitochondria on the regulation of cell homeostasis in FAOD

Mitochondria are intracellular double membrane-bound structures ubiquitous in eukaryotes and essential in the regulation of cellular homeostasis and survival (25,52,53). Their primary function is to provide energy substrates being considered the powerhouses of the cell. Furthermore, they have an important role in the regulation of apoptosis and redox homeostasis (50,54,55). Dysregulation of the metabolic pathways harbored in mitochondria can lead to mitochondrial disorders, such as FAOD. In parallel to metabolic disturbances, broad alterations in mitochondrial functionality have been reported in FAOD (8,27,46,50,51). In fact, it is accepted that the accumulated acylcarnitines and their derivatives due to defects in FAO enzymes disturb the mitochondrial homoeostasis (25).

Mitochondria are major sources of reactive oxygen species (ROS), which include free radicals such as hydroxyl radical ($HO^{\bullet}$), peroxyl radical ($RO_2^{\bullet}$) and alkoxyl radical ($RO^{\bullet}$) as well as nonradical species (hydrogen peroxide: H_2O_2) (8,56). Superoxide radical anion ($O_2^{\bullet-}$), which results from the partial reduction of O_2, and thereby ROS are mainly generated at complexes I and III of OXPHOS, being a side product of respiration (57,58). Other local of ROS production inside mitochondria is the ETF complex, by ETF and ETFDH electron leakage (58,59), which is of particular relevance in FAOD (8,59). Superoxide radical anion may react with nitric oxide (NO), produced within mitochondria, forming the radical peroxynitrite ($ONOO^{\bullet-}$). These two radicals are designated as reactive nitrogen species (RNS) (57).

ROS and RNS trigger antioxidant and protein quality control (PQC) systems to regulate their intracellular levels and maintain cellular homeostasis (55,60). Inside mitochondria, the antioxidant systems involve the action of manganese superoxide dismutase (MnSOD), peroxiredoxin (Prx III), thioredoxine (Trx II) and glutathione peroxidase (GPx), and also of mitochondrial glutathione (mtGSH). MnSOD converts $O_2^{\bullet-}$ to H_2O_2, and this molecule can be reduced to $HO^{\bullet}$ or be detoxified to H_2O by GPx and Prx III (55,57,60). Mitochondrial GSH is crucial in mitochondria homeostasis, regulating ROS generation and survival pathways. Indeed, decreased levels of mtGSH are associated with loss of mitochondrial membrane potential and release of cytochrome c (Cyt c) from mitochondria (61).
On the other hand, when the ROS and RNS levels exceed the threshold necessary for maintaining the healthy state, mitochondria and other cellular components are damaged, which triggers cellular dysfunction (57). Indeed, ROS and RNS produced at mitochondria oxidize the biomolecules nearby including mitochondrial deoxyribonucleic acid (mtDNA), phospholipids and proteins. These molecules are particularly susceptible to oxidative damage, and their function can be altered leading to mitochondrial dysfunction and, eventually to cell dysfunction and death if the damage is not repaired. Consequently, more ROS and RNS are generated and pathological processes may start due to cell dysfunction and death, in a vicious cycle (50,55,57,60). FAO-related inherited gene defects result in the accumulation of substrates and misfolded proteins and consequently in chronic oxidative stress (8). In fact, increased levels of ROS and elevated expression levels of antioxidant enzymes, such as MnSOD and peroxiredoxin-6, were reported among FAOD (8,48,62).

When mitochondria are damaged and dysfunctional, mitophagy, mitoptosis and autophagy must be activated to eliminate damaged organelles to avoid cellular dysfunction (53,63). When these mechanisms are not correctly working or are overwhelmed, cell death pathways should be activated (8,52,60). Indeed, mitochondrial damage-induced autophagy leads to preferential degradation of impaired mitochondria in a process designated mitophagy (52). This process consists on opening of permeability transition pore (PTP) in individual mitochondria, leading to depolarization of them, which are sequestered to form autophagosomes (64,65). Then, autophagosomes fuse with lysosomes to create autolysosomes, where mitochondrial digestion and degradation take place (52,66). So, autophagy can be seen as a mitochondrial quality control process, since it prevents

proliferation of defective mitochondria (52,63). Indeed, increased mitophagy was reported in RR-MADD, evidenced that mitochondria damaged by elevated ROS were eliminated by this mechanism in those patients (67). However, more studies focused on the contribution of mitophagy to the pathogenesis of FAOD are needed.

Mitoptosis is a more robust mechanism of mitochondria elimination that also protects cells from the damage caused by malfunctioning mitochondria (68,69). This process starts with fission of mitochondrial filaments into small spherical structures, leading to fragmentation of mitochondria (68). This step has been reported in apoptosis, suggesting that mitoptosis may initiate cell death when the damage of mitochondria is irreversible (70). After this, clusters of mitochondria are formed in the perinuclear region depending on cytoskeletal elements including microtubules, actin microfilaments and intermediate filaments. The clusters are occluded by a membrane to form the mitoptotic bodies, where mitochondrial decomposition takes place. The final step is protrusion of the mitoptotic bodies from the cell, releasing them into the extracellular medium (68,69). The mitoptotic program could be induced by several factors such as ATP depletion, block of respiration or depolarization of mitochondrial membrane, although overproduction of ROS has been reported as the main factor that triggers mitoptosis. ROS seem to induce PTP opening as observed in autophagy. Indeed, mitoptosis is not independent of mitophagy since autophagosomes and lysosomes are probably involved in the intermediate steps of mitoptotic body formation (68). When certain mitochondria become ROS overproducers, mitophagy is the preferential mitoptotic mechanism chosen (52,69). However, when ROS overproduction occurs in the entire mitochondrial population, mitoptosis looks like a more adequate mitoptotic mechanism (68).

When cells cannot be saved by the mitophagy or mitoptosis mechanisms, apoptosis takes over (8,52,60). The main mediators of apoptosis are caspases (cysteine-aspartic proteases), which are proteolytic enzymes that cleave inactive precursors to their active form (71,72). Caspases are a family of enzymes containing more than ten proteins divided into initiator (caspase-8 and -9) and executioner (caspase-3 and -7) ones. The initiator caspases, activated by cellular specific proteins, cleave executioner caspases which cleave protein substrates, being the executors of apoptosis (71). There are two main pathways the extrinsic and the intrinsic ones that leads to cell apoptosis (72). A schematic representation

of these apoptotic pathways is presented in figure 2, giving special attention of mitochondria-induced effectors.

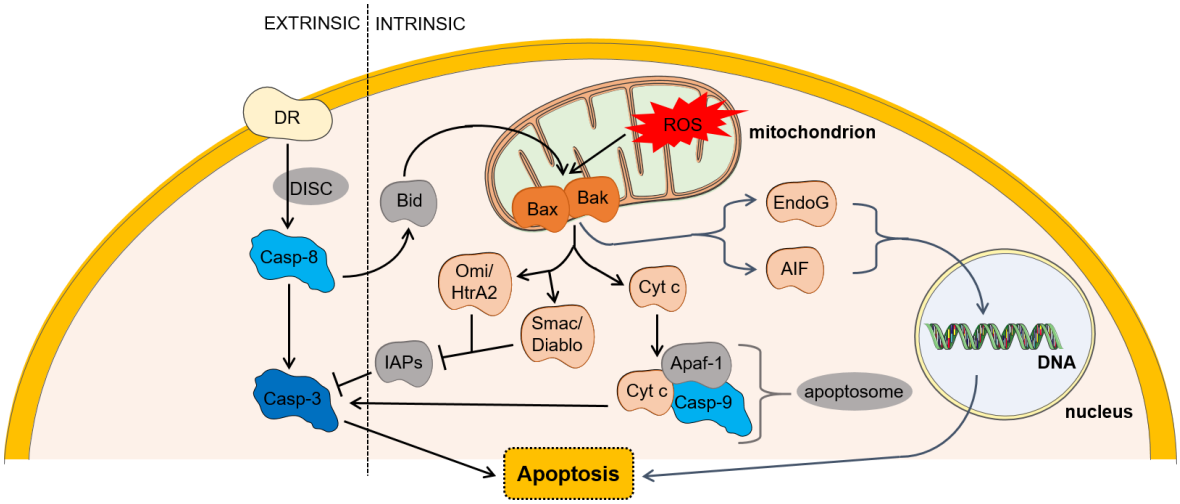

Figure 2. Extrinsic and intrinsic apoptotic pathways. The extrinsic pathway is initiated by binding of ligands to their respective DR, which leads to the formation of DISC and activates Casp-8 and this directly activates Casp-3, executing apoptosis. Casp-8 also activates Bid, starting the intrinsic pathway, which interacts with mitochondrial pro-apoptotic proteins Bax and Bak, leading to the release of several pro-apoptotic proteins, which triggers caspase-dependent (black arrows) or caspase-independent (blue arrows) cytosolic signaling events. Cyt c binds to Apaf-1 to form the apoptosome that recruits and activates Casp-9 which activates Casp-3. Caspase activation is improved by Smac/Diablo and Omi/HtrA2 since they inhibit IAPs. AIF and EndoG bind with DNA, inducing DNA fragmentation, via caspase-independent pathway. The intrinsic apoptotic pathway can also be stimulated by ROS. Figure made with *Servier Medical Art*. Abbreviations: AIF: apoptosis-inducing factor, Apaf-1: apoptotic protease-activating factor-1, Bak: bcl-2 antagonist killer 1, Bax: bcl-2 associated X protein, Bid: BH3-only pro-apoptotic protein, Casp-: caspase, number refers to the type of caspase, Cyt c: cytochrome c, DISC: death-inducing signaling complex, DNA: deoxyribonucleic acid, DR: death receptors, EndoG: endonuclease G, IAPs: inhibitor of apoptosis proteins, Omi/HtrA2: high-temperature requirement A2 serine protease, Smac/Diablo: second mitochondria-derived activator of caspases/direct IAP binding protein with low isoelectric point, ROS: reactive oxygen species.

The extrinsic pathway, also called the death receptor pathway, is initiated by binding of ligands to their respective death receptors (DR), which activates downstream signaling and leads to the formation of the death-inducing signaling complex (DISC) that culminates in the activation of caspase-8 (Figure 2). These ligands belong to the tumor necrosis factor (TNF) superfamily of cytokines and include TNFα, Fas ligand (FasL), and TNF-related apoptosis-inducing ligand (TRAIL). Activation of caspase-8 may activates directly

caspase-3 or, when caspase-8 activation is low, mediates caspase-3 activation through a process involving mitochondria (55,60,72) (Figure 2).

The second activation corresponds to the intrinsic pathway of apoptosis also designated as mitochondria-mediated pathway. Indeed, activated caspase-8 cleaves BH3-only pro-apoptotic protein (Bid), which interacts with pro-apoptotic proteins bcl-2 associated X protein (Bax) and bcl-2 antagonist killer 1 (Bak), inducing the permeabilization of the outer mitochondrial membrane and the release of pro-apoptotic proteins from mitochondria (72,73) (Figure 2). ROS, particularly H_2O_2, induce mitochondrial translocation of Bax and Bak and release of Cyt c. The more Cyt c is released from mitochondria, the more ROS are produced due to OXPHOS impairment (74). Other released proteins are second mitochondria-derived activator of caspases/direct IAP binding protein with low isoelectric point (Smac/Diablo) and apoptosis-inducing factor (AIF), which triggers caspase-dependent or caspase-independent cytosolic signaling events (73,75). Within the cytosol, Cyt c binds to apoptotic protease-activating factor-1 (Apaf-1) and ATP to form the apoptosome complex which recruits and activates the initiator procaspase-9. The activated caspase-9 activates the effector caspases-3 and -7, which execute the final steps of apoptosis (71,72). Caspase activation is improved by Smac/Diablo and high-temperature requirement A2 serine protease (Omi/HtrA2) which are crucial mitochondrial proteins for enhanced caspase activation since they antagonize the inhibitory effects of inhibitor of apoptosis proteins (IAPs) (55,60,72). The mitochondrial proteins AIF and endonuclease G (EndoG) mediate a caspase-independent apoptotic pathway by binding with deoxyribonucleic acid (DNA) and thus inducing nuclear chromatin condensation and DNA fragmentation (75,76) (Figure 2). In addition to caspase-8, the intrinsic apoptotic pathway can also be stimulated by ROS and mtDNA damage, which mediate the permeabilization of the mitochondrial outer membrane and the release of pro-apoptotic proteins (55,60) (Figure 2). In the set of FAOD there are some studies that report an overexpression of apoptotic proteins (48,49,62), including Smac/Diablo and Girdin (48) or Bax (62). So, it seems that the intrinsic pathway of apoptosis contributes to the pathogenesis of FAOD, including MADD.

1.4. The potential contribution of mitochondrial biogenesis to FAOD

The mitochondrial population constantly migrates back and forth along microtubule tracks, in which mitochondria can contact each other end to end and fuse. This mitochondrial dynamics, including mitochondrion movement and change of shape and size, is regulated by fusion and fission mechanisms (50,77). Since the discovery of the *Drosophila* mitofusin gene (Fzo) in 1997 by Hales and Fuller (78), there have been rapid advances in the knowledge of the molecular basis of mitochondrial fusion and fission.

The fusion mechanism is regulated by mitofusins (Mfns), which exist in two identical isoforms in mammals, Mfn1 and Mfn2, and localize in the outer mitochondrial membrane. (77,79). Several studies demonstrated that cells lacking Mfns or mitochondrial dynamin-like 120 kDa protein (OPA1), located within the mitochondrial intermembrane space, present reduced levels of mitochondrial fusion (80–82). Indeed, when both Mfn1 and Mfn2 are absent, there is no mitochondrial fusion, resulting in the complete loss of mitochondrial tubules and thus in a dramatic decreased mitochondrial functionality (81). Consequently, mitochondrial fusion is necessary for the normal function of cells, and perturbations in this process might lead to diseases development (77). The fission mechanism involves dynamin-related protein 1 (Drp1) and mitochondrial fission 1 protein (Fis1) (77,83,84), although other proteins such as endophilin B1 and mitochondrial membrane protein 18 (MTP18) seem to be involved in this process too (85,86). Indeed, decreased amounts of these proteins result in elongation of mitochondrial tubules. These abnormalities in mitochondrial morphology are suggestive of defects in fission mechanism (83–86). Changes in the regulation of these processes leading to impaired mitochondrial functionality have been reported in FAOD (62,67,87). In fact, a down-regulation of Mfn2 was found in RR-MADD patients (67).

Mitochondrial biogenesis is regulated by many genes related to cellular energy state and stress level (50), such as peroxisome proliferator-activated receptor γ coactivator 1 alpha (PGC-1α) (88,89). Indeed, all the members of the PGC-1 family (PGC-1α, PGC-1β and PGC-1-related coactivator) have been associated with mitochondrial biogenesis, playing a central role in this process (54,90–93). These proteins are key regulators of mitochondrial content and oxidative metabolism, being also critical in the regulation of glucose, lipid, and

energy homeostasis (89,90). In figure 3 a schematic representation of the regulation of mitochondrial biogenesis by PGC-1α signaling is presented.

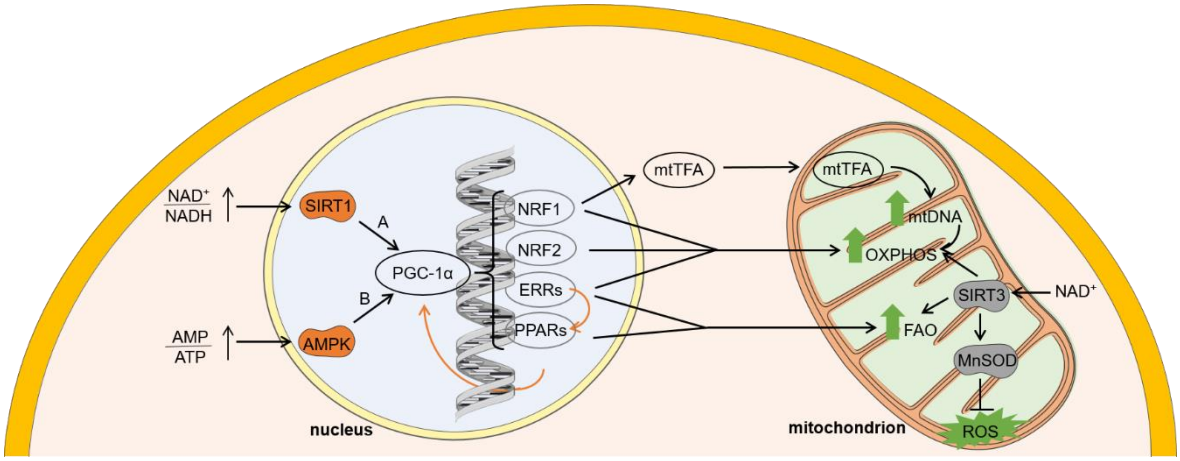

Figure 3. Regulation of mitochondrial biogenesis by PGC-1α signaling. Enhanced NAD^+/NADH ratio stimulates SIRT1 which deacetylates PGC-1α, whereas the increase in AMP/ATP ratio activates AMPK which phosphorylates it. Both deacetylation (A) and phosphorylation (B) activate PGC-1α, leading to stimulation of specific nuclear factors, such as NRFs, ERRs and PPARs, which activate their target genes. NRF1 regulates mtTFA which increases mtDNA gene transcription and replication. This and both NRFs and ERRs lead to increase in OXPHOS. ERRs also stimulate FAO and PPAR which has the same effect. SIRT3, in NAD^+-dependent via, stimulates OXPHOS, FAO and ROS metabolism proteins. All these processes lead to mitochondrial biogenesis. Figure made with *Servier Medical Art*. Abbreviations: AMP: adenosine monophosphate, AMPK: AMP-activated protein kinase, ATP: adenosine triphosphate, ERRs: oestrogen-related receptors, FAO: mitochondrial fatty acid β-oxidation, MnSOD: manganese superoxide dismutase, mtDNA: mitochondrial deoxyribonucleic acid, mtTFA: mitochondrial transcription factor A, NAD^+: nicotinamide adenine dinucleotide, NADH: reduced form of NAD^+, NRFs: nuclear respiratory factors, OXPHOS: oxidative phosphorylation, PGC-1α: peroxisome proliferator-activated receptor γ coactivator 1 alpha, PPARs: peroxisome proliferator-activated receptors, ROS: reactive oxygen species, SIRT1: sirtuin 1, SIRT3: sirtuin 3.

PGC-1α is a powerful regulator of multiple aspects of mitochondrial gene expression, inducing mitochondrial biogenesis and uncoupled respiration (89,91). This protein requires transcription factors for the trans-activation of mitochondrial biogenesis genes. Among these are the nuclear respiratory factors 1 and 2 (NRF1 and NRF2), peroxisome proliferator-activated receptors (PPARs) and others (89,91) (Figure 3). PPARs have different subtypes (α, β/δ and γ) that can be stimulated by pharmacological activation and are responsible for tissue-specific activation of PGC-1α gene expression (54). NRFs

activate the transcription of many genes involved in the respiratory chain function like the Cyt c and regulate the mitochondrial transcription factor A (mtTFA). This protein is a nuclear factor that acts in the mtDNA, stimulating its replication and transcription (89,91) (Figure 3). The expression of other genes including ATP synthase, MnSOD and glutathione peroxidase-1 was also increased in cells expressing PGC-1α and PGC-1β (89,92). PGC-1α and PGC-1β lead to a similar overexpression of many mitochondrial genes, although PGC-1β preferentially induces certain genes involved in the cytosolic ROS removal, such as light and heavy subunits of γ-glutamylcysteine synthetase (92).

The activity of PGC-1α is regulated by post-translational modifications such as acetylation and phosphorylation (89). Adenosine monophosphate-activated protein kinase (AMPK) is one of the main regulator of cellular metabolism and there has been reported an association between the activation of AMPK and the increase in gene expression of PGC-1α and mitochondrial proteins (Figure 3), such as Cyt c and mitochondrial uncoupling protein 2 (UCP2) (89,91,94). Indeed, the increase in PGC-1α may be reached by direct phosphorylation of PGC-1α on specific amino acids by AMPK or by binding proteins, such as cyclic adenosine monophosphate response element-binding protein and thyroid hormones, that bind to specific domains localized inside of the PGC-1α promoter and thus stimulating its transcription. AMPK is activated by an increase in adenosine monophosphate (AMP) levels (54,89). (Figure 3). There are other kinases involved in PGC-1α regulation, including the protein kinase A (PKA) and the p38 mitogen-activated protein kinase (MAPK) (95,96). The PKA pathway is stimulated by increased intracellular levels of cyclic adenosine monophosphate (cAMP) that activate PKA, which consequently phosphorylates and activates sirtuin 1 (SIRT1). SIRT1 activates PGC-1α, leading to increased expression of FAO genes (95). Activation of the p38 MAPK pathway stimulates upstream transcription factors of the *PGC-1α* gene, thus enhancing its promoter activity and leading to increased PGC-1α mRNA levels (96).

Sirtuins are deacetylases that regulate responses to a variety of stresses, like calorie restriction and metabolic stress, via NAD^+-dependent deacetylation (97). Sirtuin 3 (SIRT3) is located into mitochondria where it regulates the acetylation levels of a large range of substrates including proteins from FAO, OXPHOS and ROS metabolism (98,99) (Figure 3), although the exact mechanism is still somewhat unclear (54). Mice lacking SIRT3 exhibit hallmarks of FAOD like reduced ATP levels during fasting. Interestingly, these

mice showed accumulation of long-chain acylcarnitines and TG, suggesting that oxidation of long-chain acyl substrates was impaired. However, this defect appeared to be specific, because citrate synthase (CS) activity, an indicator of mitochondrial function, was not altered. Indeed, the long-chain acyl-CoA dehydrogenase (LCAD) in these mice was not deacetylated during fasting, which results in reduced enzymatic activity of LCAD. These findings indicate that SIRT3 is necessary for LCAD deacetylation, particularly of lysine forty-two on its amino acids chain. So, reversible deacetylation of mitochondrial enzymes by SIRT3 may be considered a novel metabolic regulatory mechanism for FAO (98). In addition to this study, others focused on SIRT1 demonstrated the importance of deacetylation mechanism as a modulator of mitochondrial metabolism (100,101). SIRT1 also enhances FAO protecting against diet-induced metabolic disorders (100). Some studies have demonstrated an association of these proteins with FAOD pathogenesis (67,102). Indeed, it was reported a down-regulation of SIRT3 (67) and an overexpression of peroxisome proliferator-activated receptor α (PPARα) (102) in RR-MADD patients.

2. Aims

The aim of the present study was to characterize the mitochondrial dynamics in multiple acyl-CoA dehydrogenase deficiency (MADD) in order to better understand the molecular mechanisms underlying the disease pathogenesis. In this way, it was our purpose to evaluate the contribution of mitochondrial biogenesis, metabolic remodeling and antioxidant defense mechanisms to MADD phenotype, in fibroblasts isolated from skin biopsies of patients with distinct clinical outcomes. Other biological processes such as autophagy and apoptosis were also evaluated. The integration of all data added new insights on the understanding of the molecular pathways underlying the large range of phenotypes observed in MADD patients, which may eventually lead to the identification of molecular targets for more efficient therapeutic strategies.

3. Materials and Methods

3.1. Experimental design

In order to fulfill the aim of this study, the sequential steps described in figure 4 were followed. Immunoblotting, immunocytochemistry and spectrophotometric assessment of enzymatic activities were the experimental procedures selected to better understand the mitochondrial dynamics in multiple acyl-CoA dehydrogenase deficiency (MADD).

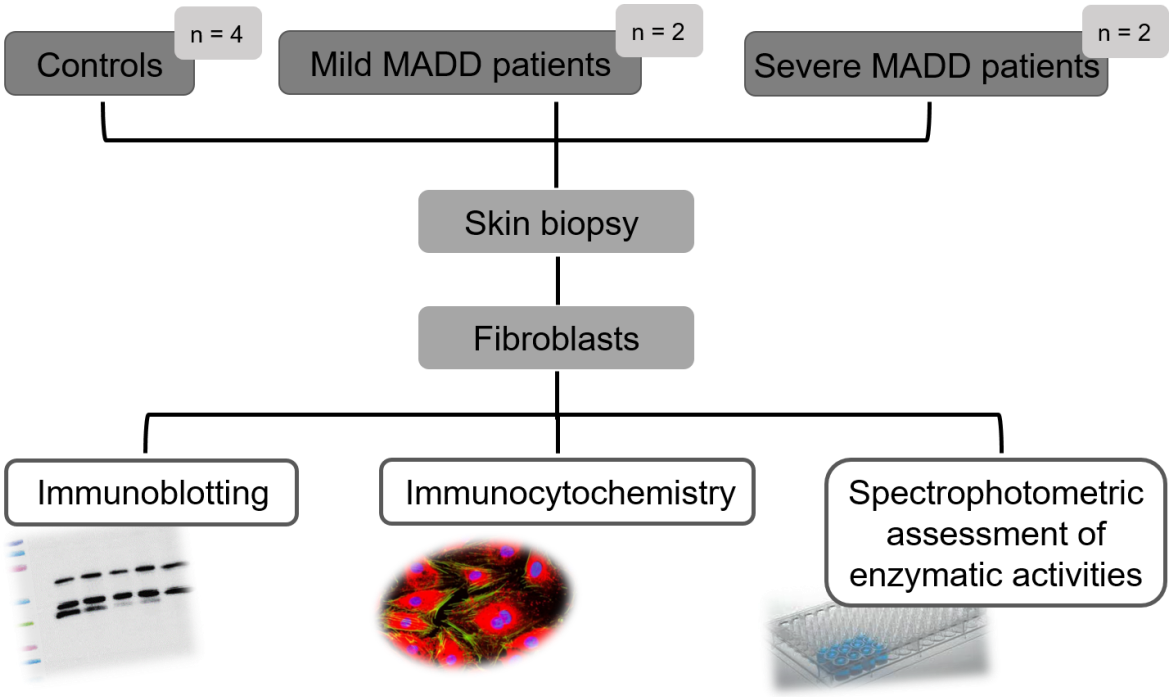

Figure 4. Experimental design followed at the present work. Skin biopsy was done in all MADD patients and controls (heathy individuals aged-matched with patients) to obtain cultured fibroblasts. These cells were then analyzed by immunoblotting to semi-quantify the amount of specific proteins, by immunocytochemistry to estimate the mitochondrial density and by specific spectrophotometric assays to measure the activity of key metabolic enzymes.

3.2. Samples characterization

Samples from four MADD patients and four healthy individuals, with no apparent related disease and aged-matched, were used. All the patients presented mutations in the *ETFDH* gene and are non-responsive to riboflavin therapy. Two patients presented mild forms of MADD (MADD1 and MADD2), while the other two (MADD3 and MADD4) had severe forms. The MADD1 and MADD2 patients are both homozygous for the mutation p.R175H

in *ETFDH*, corresponding to the well described late onset form (type III) of MADD. The MADD3 patient is homozygous for the mutation p.X618QextX14 in *ETFDH* while MADD4 patient is compound heterozygous for p.X618QextX14 and p.E412X, also in *ETFDH*. These two patients (MADD3 and MADD4) phenotypically correspond to the early onset form of MADD. Both controls and patients samples were used, anonymously, after each subject/legal guardian gave written informed consent.

3.3. Cell culture and cell extracts preparation

Skin fibroblasts from MADD patients and healthy individuals (controls) were grown in Dulbecco's Modified Eagle Medium (DMEM 21885, Gibco™, Thermo Fischer Scientific®) supplemented with 10 % fetal calf serum, 1 % penicillin, streptomycin and fungizone in 75 cm^2 culture flasks at 37 ºC in a 5 % CO_2 incubator. Three culture flasks from each sample, corresponding approximately to 10^3 cells, were grown to pre-confluence status. The pellets of cultured fibroblasts were dissolved in lysis buffer (100 mM potassium phosphate, pH 7.4, 0.1 % (v/v) Triton X-100) and then the cell suspension was homogenized in a tight-fitting Potter-Elvejhelm. The final solution was stored at -80 ºC for further analyzes.

3.4. Total protein quantification

An aliquot of cell homogenate was used for total protein quantification using the commercial kit *DC Protein Assay* (Bio-Rad®, Hercules, CA, USA). This kit is based on Lowry *et al.* (103) assay, on which proteins react with copper in an alkaline solution and then occurs the reduction of Folin reagent by the copper-treated protein, leading to the formation of a blue color with maximum absorbance at 750 nm. In this way, a calibration curve with standard solutions of bovine serum albumin (BSA) at concentrations between 0.312 and 10 mg/mL was made. Equal volumes (5 μL) of sample or standard were used for the experimental procedure according to manufacturer's recommendations and the absorbance was read at 750 nm in a microplate reader (Multiskan GO, Thermo Fischer Scientific®, Northumberland, UK).

3.5. Protein precipitation

The amount of total protein in cell extracts of patient MADD4 was much lower than in the other samples. So, before the analysis of this sample by sodium dodecyl sulphate-polyacrylamide gel electrophoresis (SDS-PAGE), protein was precipitated. Briefly, the sample volume corresponding to 20 μg of protein was dissolved in four times that volume of cold acetone (-20 ºC) and then incubated overnight at -20 ºC. After that, the sample was centrifuged 10 minutes at 17,000x*g* and 4 ºC and then the supernatant was discharged. The protein pellet was allowed to dry at room temperature and finally dissolved in 0.5 M Tris-HCl pH 6.8.

3.6. SDS-PAGE and Western blotting

To analyze the expression of target proteins, equal amounts of protein (20 μg) from each sample were dissolved in loading buffer (0.5 M Tris-HCl pH 6.8, 4 % (w/v) SDS, 15 % (v/v) glycerol, 1 mg/mL bromophenol blue and 20 % (v/v) β-mercaptoethanol) and heated 5 minutes at 100 ºC and then loaded in a 12.5 % SDS-PAGE gel prepared according to Laemmli (104). The gels were run for 45 minutes at 180 V in running buffer (250 mM glycine, 25 mM Tris, pH 8.6 and 0.1 % (w/v) SDS). The resolved proteins were transferred to a nitrocellulose membrane (Amersham™ Protran™, GE Healthcare, Germany, 0.45 μm porosity) for 2 hours at 200 mA. The buffer used contained 192 mM glycine, 25 mM Tris, pH 8.3 and 20 % (v/v) methanol and the efficacy of transfer was confirmed by Ponceau S staining. After that, membranes were blocked in order to avoid unspecific binding with 5 % (w/v) nonfat dry milk in Tris-buffered saline (TBS) with Tween 20 (TTBS; 100 mM Tris, 1.5 mM NaCl, pH 8.0 and 0.05 % (v/v) Tween 20) for 1 hour at room temperature with shaking. Next, the membranes were incubated with the primary antibody, diluted 1:1000 in 5 % (w/v) nonfat dry milk in TTBS for 2 hours at room temperature or overnight at 4 ºC. The primary antibodies used were rabbit monoclonal anti-APG5L/ATG5 (ab108327), rabbit monoclonal anti-Bax (ab32503), rabbit monoclonal anti-Bcl2A1 (ab33862), rabbit polyclonal anti-ETFDH (ab91508), rabbit polyclonal anti-GAPDH (ab9485), rabbit polyclonal anti-MnSOD (ab13533), rabbit polyclonal anti-mtTFA (ab47548) and rabbit polyclonal anti-PGC1 alpha (ab54481) from Abcam (Cambridge,

UK), rabbit monoclonal anti-Caspase-3 cleaved (9664S) and rabbit monoclonal anti-SirT3 (2627S) from Cell Signaling Technology (MA, USA) and rabbit polyclonal anti-Atpalpha (GTX123137) from GeneTex Inc. (US). Following, the membranes were washed three times (10 minutes each) with TTBS to remove the unbind antibodies. Next, the membranes were incubated with the appropriate secondary horseradish peroxidase-conjugated antibody (anti-mouse or anti-rabbit, NA931 or NA934, respectively; GE Healthcare, UK), diluted 1:1000 with 5 % (w/v) nonfat dry milk in TTBS, for 1 hour at room temperature with shaking. The membranes were washed three times (10 minutes each) again with TTBS and exposed with enhanced chemiluminescence ECL reagent (WesternBright™ ECL, advansta, CA, USA) followed by exposure to X-ray films (Kodak Biomax Light Film, Sigma®, St. Louis, USA). Film images were acquired using GelDoc XR system (Bio-Rad®, Hercules, CA, USA) and semi-quantitative analysis of optical density (OD) was performed with QuantityOne® 1-D Analysis Software version 4.6.3 (Bio-Rad®, Hercules, CA, USA). Exceptionally, for ATG5 protein the detection method used was the fluorescent one since this technique is more sensitive than chemiluminescence. So, the secondary antibody used was fluorophore-conjugated (goat anti-rabbit 926-68071 diluted 1:5000 in 5 % (w/v) nonfat dry milk in TTBS) and after the third wash with Tris-buffered saline (TBS; 100 mM Tris, 1.5 mM NaCl, pH 8.0) instead of TTBS, the fluorescence of membranes was automatically measured using the Odyssey Infrared Imaging System (LI-COR® Biosciences, US).

3.7. Determination of the content of carbonylated proteins by Slot-blot

The content of carbonyl groups in proteins was evaluated according to Robinson *et al.* (105) with some modifications. Firstly, a given volume (V) from each sample containing 10 μg of protein was mixed with 12 % (w/v) SDS (V) and 20 mM 2,4-dinitrophenylhydrazine (DNPH) prepared in 10 % (v/v) trifluoroacetic acid (2V). The reaction between carbonyl groups and DNPH leads to the formation of 2,4-dinitrophenil (DNP) hydrazone which can be detected by immunoblotting. Next, sample mixtures were incubated in the dark at room temperature for 30 minutes. The addition of 2 M Tris with 18 % (v/v) β-mercaptoethanol (1.5V) stopped the reaction. Two different dilutions, 1:75 and 1:100, were prepared in TBS. After this, 100 μL of each sample dilution were transferred

to a nitrocellulose membrane (Amersham™ Protran™, GE Healthcare, Germany, 0.45 μm porosity) using a Slot-blot system, according to manufacturer's instructions. The nitrocellulose membranes were first activated by immersion on 10 % (v/v) methanol solution for 5 seconds and placed in distilled water until transference procedure. The immunodetection was performed as described above for Western blotting. The primary antibody used (mouse monoclonal anti-DNP; MAB2223, Millipore) was diluted 1:1000 in 5 % (w/v) nonfat dry milk in TTBS and incubated for 1 hour at room temperature with shaking.

3.8. Immunocytochemistry

Immunocytochemistry was performed to obtain information about mitochondrial density in cultured fibroblasts from MADD patients. Briefly, fibroblasts were grown in coverslips inside 6-well plates at 37 ºC in a 5 % CO_2 incubator until they reach approximately a 60 % confluence. At that time, the culture medium (see section 3.3) was removed and fibroblasts were washed twice in Phosphate-buffered saline (PBS, P4417-100TAB, Sigma®; 0.01 M phosphate buffer, 0.0027 M potassium chloride, 0.137 M sodium chloride, pH 7.4) and fixed for 10 minutes at room temperature with 3.7 % (v/v) formaldehyde solution prepared in PBS. After fixation, fibroblasts were washed three times (10 minutes each) with PBS. Coverslips were stored at 4 ºC in PBS overnight due to convenience issues. In the next day, fibroblasts were permeabilized for 10 minutes with 0.2 % (v/v) Triton X-100 in PBS and then washed three times (10 minutes each) with PBS. Nonspecific binding was blocked with blocking solution (5 % (w/v) BSA and 1 % (w/v) goat serum in PBS) for 30 minutes. After wash with PBS, fibroblasts were incubated with rabbit polyclonal anti-COX IV (ab16056, Abcam, Cambridge, UK) diluted 1:1000 in blocking solution at room temperature for 1 hour in a wet chamber. Fibroblasts were then washed three times (10 minutes each) with PBS and incubated with the secondary antibody diluted 1:500 in blocking solution at room temperature for 30 minutes in a dark and wet chamber. The antibody used was goat anti-rabbit Alexa Fluor® 594 (A-11037, Thermo Fischer Scientific®). After three washes (10 minutes each) with PBS, coverslips were incubated with 50 μL of Hoechst 33258 (Polysciences Europe GmbH, Eppelheim, Germany) diluted 1:8000 for 1 minute at room temperature in a dark and wet chamber to stain the nuclei.

Then, two washes with PBS and one with distilled water (10 minutes each) were done and fibroblasts were mounted on the slide with Mowiol 4-88 (Sigma-Aldrich Química) and they were let to dry. Slides were stored protected from the light at 4 ºC. Images were acquired using an Olympus IX-81 inverted epifluorescence microscope (Olympus Portugal–Opto-Digital Tecnologias, S.A., Lisboa, Portugal), with a x100 objective.

3.9. Spectrophotometric activity assays

3.9.1. ATP synthase activity

The activity of respiratory chain complex V was measured according to Simon *et al*. (106). The phosphate produced by hydrolysis of ATP reacts with ammonium molybdate in the presence of reducing agents to form a blue color complex. The intensity of this complex is proportional to the concentration of phosphate in solution. Equal volumes (15 μL) from each sample were dissolved in reaction buffer (0.2 M KCl, 3 mM $MgCl_2$, 10 mM Tris-HCl, pH 8.4) and incubated at 30 ºC for 1 minute. Then an equal volume of 0.1 M ATP was added and incubated for 1 minute at 30 ºC. The reaction was stopped by the addition of 30 μL of 3 M tricloroacetic acid. After centrifugation at 9,000x*g* and 4 ºC for 10 minutes, 125 μL of supernatant were mixed with 625 μL of test solution (0.37 M H_2SO_4, 0.01 M ammonium molybdate and 0.1 M ferrous sulphate) and then incubated for 15 minutes at room temperature. In parallel, a calibration curve with standard solutions of potassium dihydrogen phosphate (KH_2PO_4) at concentrations between 0.0 and 1.0 mM were prepared. Oligomycin was used as an ATP hydrolase inhibitor. The absorbance was read at 610 nm in a microplate reader (Multiskan GO, Thermo Fischer Scientific®, Northumberland, UK). Then, the absorbance values were converted to concentration (mM) per minute from the equation of calibration curve and then divided by total protein in order to obtain the enzymatic activity values (mmol $Pi.min^{-1}.mg^{-1}$) on each sample.

3.9.2. Citrate synthase activity

The activity of citrate synthase was determined according to Coore *et al.* (107). This method evaluates the presence of free thiol groups in CoASH by its reaction with 5,5'-dithiobis-(2-nitrobenzoate) (DTNB). The resulting 2-nitro-5-thiolbenzoate (TNB) anion has a strong absorption at 412 nm, allowing the reaction to be followed spectrophotometrically. Firstly, the reaction mixture including 200 mM Tris buffer pH 8.0, 10 mM acetyl-CoA, 10 mM DTNB and 0.1 % (v/v) Triton X-100 was prepared. Then, equal volumes (5 μL) from each sample (except for MADD4 for which the volume used was 10 μL) were incubated with 190 μL (185 μL for MADD4) of reaction mixture and the absorbance was read at 412 nm for approximately 2 minutes at 30 ºC in a microplate reader (Multiskan GO, Thermo Fischer Scientific®, Northumberland, UK). Then, equal volumes (5 μL) of 10 mM oxaloacetate were added to each well of the microplate and the absorbance was again read at 412 nm for approximately 2 minutes at 30 ºC. The absorbance values of the last assay were plotted against time and the slope of the equation ((ΔA412)/min) was divided by the extinction coefficient of TNB at 412 nm (13.6 $mM^{-1}.cm^{-1}$). Finally, the values obtained were divided by total protein in order to obtain the enzymatic activity values ($nmol.min^{-1}.mg^{-1}$) on each sample.

3.10. Statistical analysis

All the data is presented as mean ± standard deviation (SD) of replicates of n = 4 for controls and replicates for each patient. The statistical analysis between MADD patients and controls was performed using the unpaired students *t*-test from GraphPad Prism® software for Windows (version 6.0). The level of significance was set at 5 % (*p*-value < 0.05).

4. Results

4.1. Analysis of ETFDH expression

To characterize the expression of electron transfer flavoprotein dehydrogenase (ETFDH) in MADD patients and relate it with the mutation in the *ETFDH* gene, Western blotting was performed. The results of ETFDH expression obtained for the controls and MADD patients are presented in figure 5.

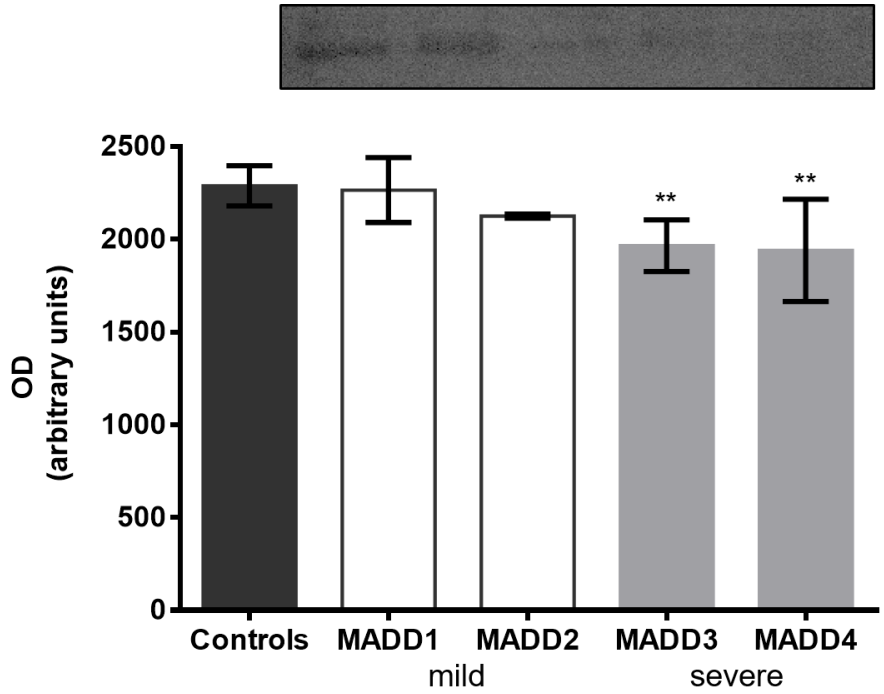

Figure 5. Expression levels of ETFDH measured by Western blotting in total homogenates of skin fibroblasts from controls and MADD patients. MADD1 and MADD2 correspond to a mild form while MADD3 and MADD4 have severe form of MADD. Above the graph is presented a representative image of the Western blots obtained. The values (mean ± SD) are expressed in arbitrary units of optical density (OD). ** $p < 0.01$.

Only patients with the severe form of MADD (MADD3 and MADD4) presented a significant difference on ETFDH expression levels compared to controls ($p < 0.01$). This is in accordance with what is expected based on the nature of the disease-causing genotype. The mutation p.E412X leads to a truncated protein and p.X618QextX14 to an extended protein that are most probably degraded/partially degraded by cell PQC system. Mild patients (MADD1 and MADD2) are homozygous for a missense mutation that although impairing ETF/ETFDH complex functionality, did not result in a significant decrease of ETFDH expression levels.

4.2. Effect of MADD on cells' metabolic status

The ETFDH enzyme links the β-oxidation with the oxidative phosphorylation (OXPHOS) through the transfer of electrons from acyl-CoA dehydrogenases to ubiquinone (CoQ) (14). In order to evaluate the impact of this enzyme's deficit or non-functionality, the levels of glyceraldehyde-3-phosphate dehydrogenase (GAPDH), and the levels and activity of ATP synthase were measured. Figure 6 presents the results obtained.

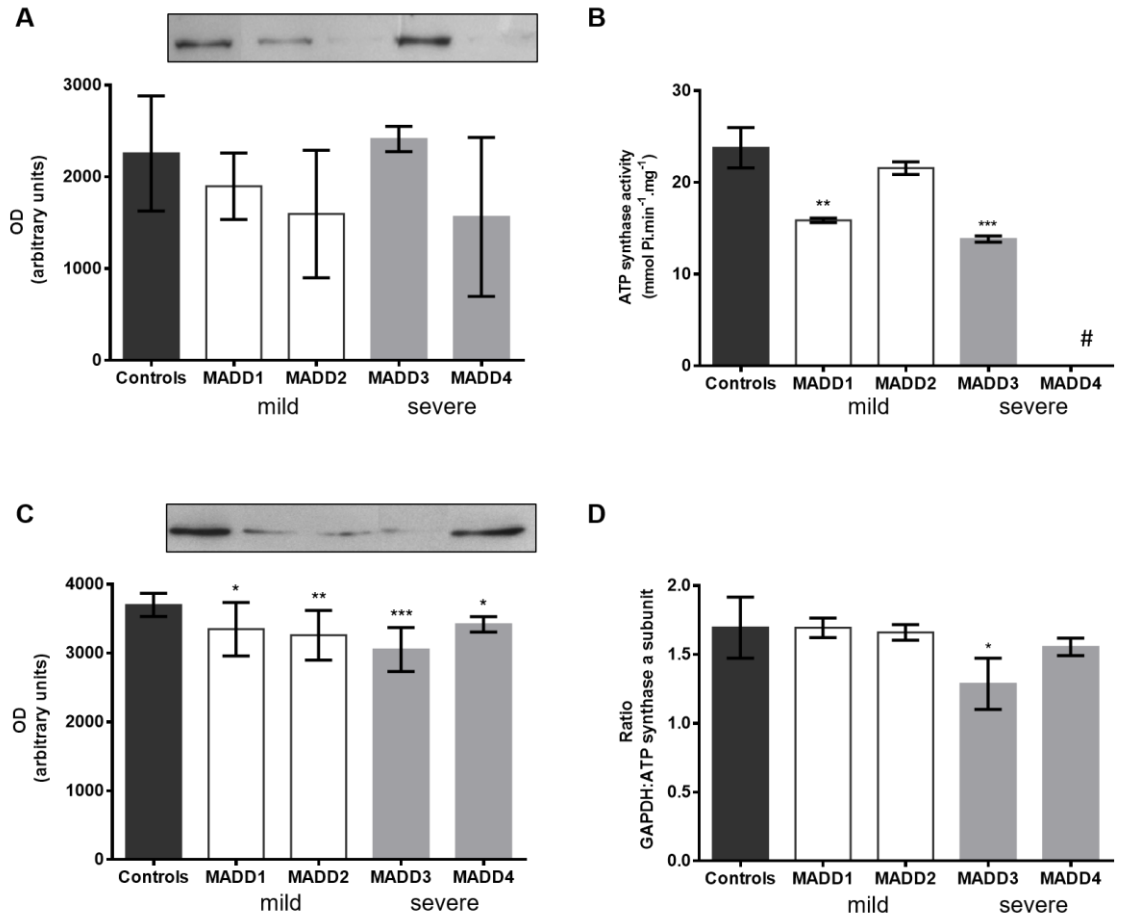

Figure 6. Effect of ETFDH deficiency on the metabolic status of skin fibroblasts' homogenate. MADD1 and MADD2 correspond to a mild form while MADD3 and MADD4 have severe form of MADD. Expression levels of ATP synthase α subunit measured by Western blotting; above the graph is presented a representative image of the Western blots obtained (**A**). ATP synthase activity was spectrophotometrically measured and values are expressed in mmol $Pi \cdot min^{-1} \cdot mg^{-1}$ (**B**). Expression levels of GAPDH measured by Western blotting; above the graph is presented a representative image of the Western blots obtained (**C**). Ratio between GAPDH and ATP synthase α subunit (**D**). The values (mean ± SD) are expressed in arbitrary units of optical density (OD) for A and C. * $p < 0.05$; ** $p < 0.01$; *** $p < 0.001$. # The value obtained for this sample was below the detection limit so the value is hide in the graph.

Western blotting analysis of ATP synthase α subunit showed no significant differences for MADD patients compared to controls, despite a tendency towards reduced levels for MADD1, MADD2 and MADD4 (Figure 6-A). The activity of ATP synthase was also measured, and lower values were noticed for all patients with the exception of MADD2 (Figure 6-B). Unfortunately for MADD4 the ATP synthase activity was not possible to measure because of the low protein concentration levels obtained in the samples.
Curiously, the protein levels of GAPDH were significantly lower in all patients compared to controls (Figure 6-C). When the ratio between GAPDH and ATP synthase α subunit expression levels was calculated, no significant differences among MADD patients and controls were observed, except for MADD3 who showed significantly lower values than controls ($p < 0.05$, Figure 6-D).

4.3. Effect of MADD on oxidative stress

In order to evaluate the oxidative status in MADD, protein carbonylation was assessed by Slot-blot. In parallel, the axis sirtuin 3 (SIRT3) - manganese superoxide dismutase (MnSOD) was studied by Western blotting. In figure 7 are showed the results obtained for MADD patients and controls.

Data evidenced no alterations in the content of carbonylated proteins (Figure 7-A). For the other hand, SIRT3 levels were significantly lower in MADD patients compared to controls, except for MADD1 (Figure 7-B). In opposite, no significant differences were observed for the MnSOD levels (Figure 7-C). However, a significant decrease of MnSOD was noticed for MADD3 compared to controls ($p < 0.001$).

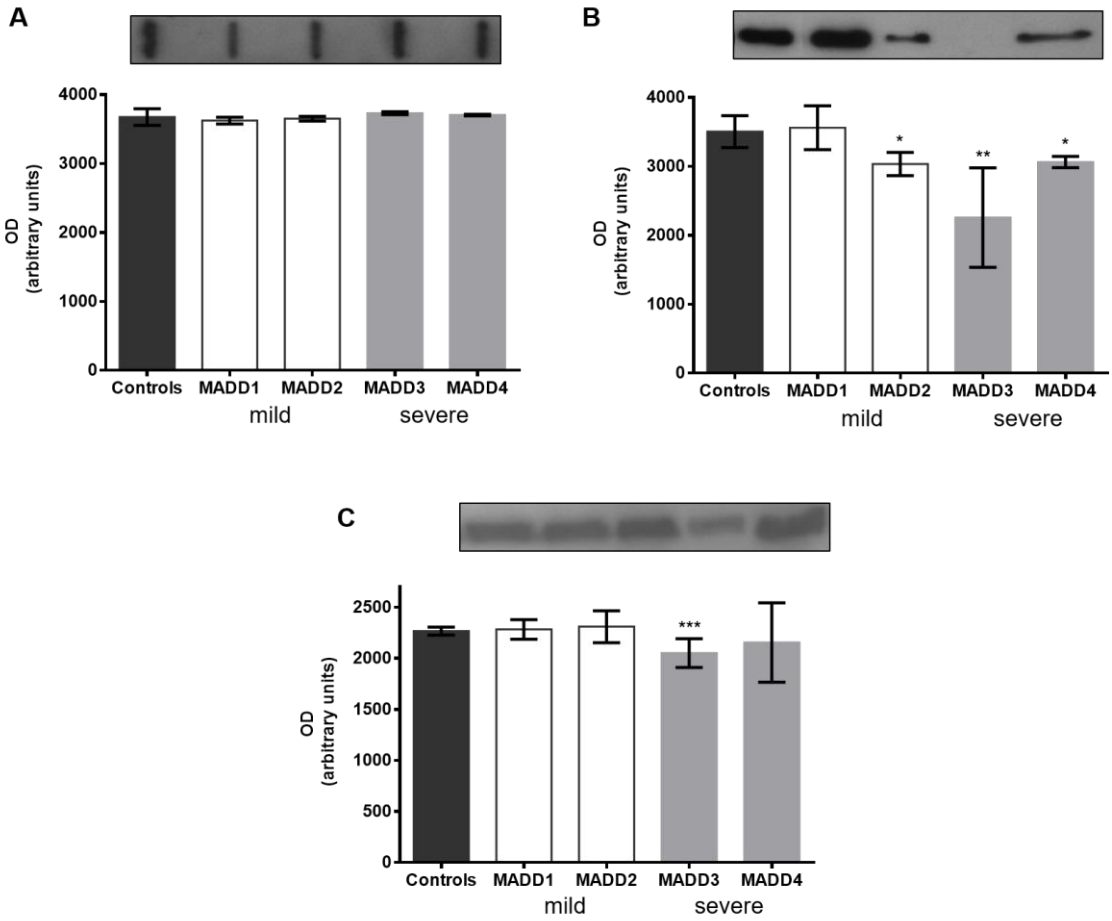

Figure 7. Effect of ETFDH deficiency on protein carbonylation (**A**), SIRT3 (**B**) and MnSOD (**C**) levels in total homogenates of skin fibroblasts assessed by immunoblotting. MADD1 and MADD2 correspond to a mild form while MADD3 and MADD4 have severe form of MADD. Above each graph is presented a representative image of the immunoblots obtained. The values (mean ± SD) are expressed in arbitrary units of optical density (OD). * $p < 0.05$; ** $p < 0.01$; *** $p < 0.001$.

4.4. Effect of MADD on mitochondrial biogenesis and mitophagy

In order to characterize the mitochondrial dynamics in MADD pathogenesis, protein markers of mitochondrial biogenesis and mitophagy were selected to be evaluated. The activity of the mitochondrial enzyme citrate synthase (CS) was spectrophotometrically assessed once this enzyme is considered a rough indicator of the number of mitochondria content on cells (108). The expression levels of the mitochondrial transcription factor A (mtTFA) and its regulator peroxisome proliferator-activated receptor γ coactivator 1 alpha

(PGC-1α) were measured by Western blotting. Figure 8 presents the results of the mitochondrial dynamics analysis obtained for MADD patients and controls.

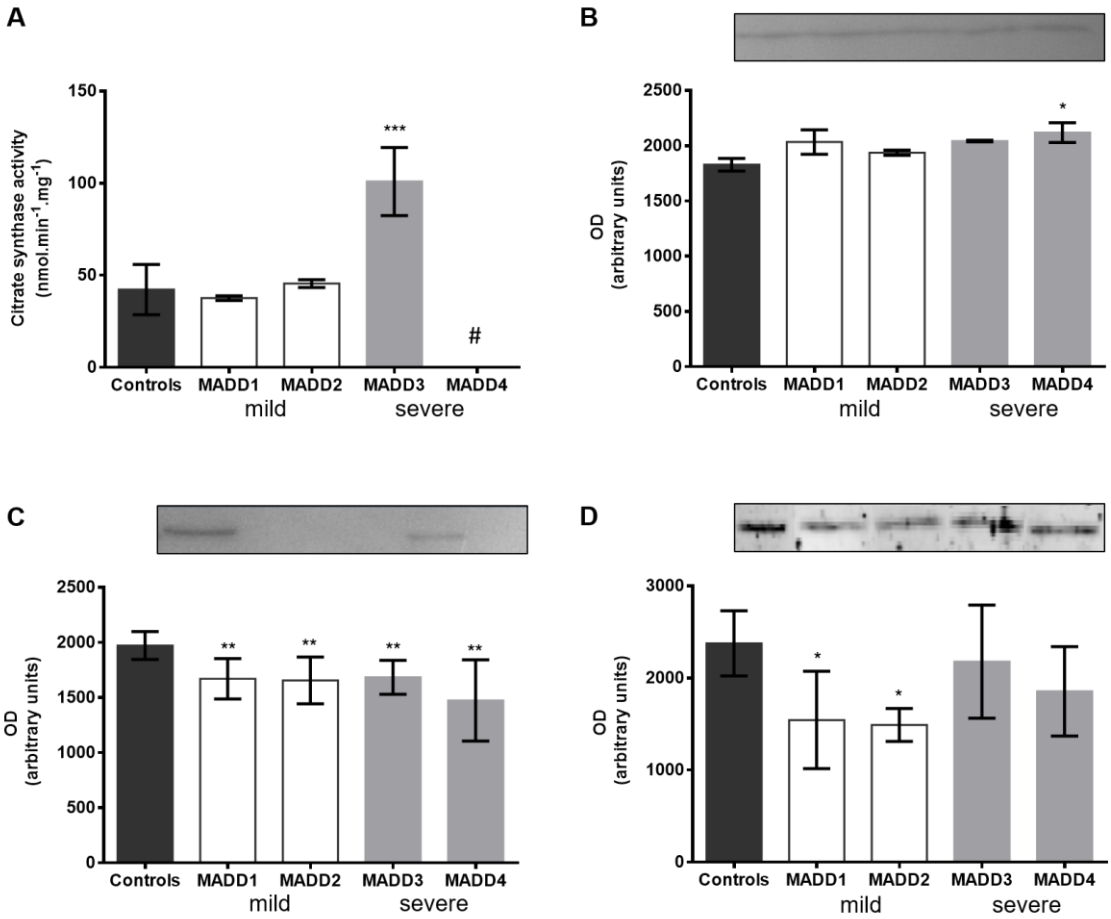

Figure 8. Effect of ETFDH deficiency on mitochondrial biogenesis and mitophagy markers assessed in total homogenates of skin fibroblasts. MADD1 and MADD2 correspond to a mild form while MADD3 and MADD4 have severe form of MADD. Citrate synthase activity was spectrophotometrically measured and the values (mean ± SD) are expressed in $nmol \cdot min^{-1} \cdot mg^{-1}$ (**A**). Expression levels of mtTFA (**B**), PGC-1α (**C**) and ATG5 (**D**) measured by Western blotting; above each graph is presented a representative image of the Western blots obtained. The values (mean ± SD) are expressed in arbitrary units of optical density (OD) for B, C and D. * $p < 0.05$; ** $p < 0.01$; *** $p < 0.001$. # The value obtained for this sample was below the detection limit so the value is hide in the graph.

The activity of CS was 2-fold higher in MADD3, compared to controls ($p < 0.001$; Figure 8-A). No significant CS activity differences were noticed for mild MADD patients. Unfortunately, we were unable to measure CS activity in MADD4 due to the low protein concentration in the corresponding samples. The levels of mtTFA were only significantly

higher in MADD4 ($p < 0.05$; Figure 8-B), although some tendency towards increased levels was noticed for the other MADD patients. Protein levels of PGC-1α were significantly lower in all MADD patients than in controls ($p < 0.01$; Figure 8-C). So, data suggest that mitochondrial biogenesis is down-regulated in MADD patients despite the higher levels of mtTFA detected in a patient with a severe phenotype.

The contribution of autophagy to mitochondrial dynamics was assessed by measuring the content of autophagy protein 5 (ATG5) by Western blotting. Significantly lower levels were observed in mild MADD patients compared to controls ($p < 0.05$; Figure 8-D), without significant differences noticed for patients with the severe phenotype (MADD3 and MADD4).

In addition to the analysis of these proteins detected by Western blotting, immunocytochemistry was also applied to estimate the mitochondrial density (preliminary studies). This was done targeting subunit IV of cytochrome c oxidase (COX IV), which localizes in the inner mitochondrial membrane and is ubiquitous in human tissues. This subunit is essential for cytochrome c oxidase (C-IV) assembly and functionality and thus for oxidative phosphorylation (109). The results from immunofluorescence are presented in figure 9.

The immunofluorescence images obtained for COX IV suggest that both mild and severe MADD patients apparently have COX IV in a more restricted area compared to controls. Patients present small dots more intense near the nucleus, while in the controls they are more spread alongside the fibroblasts (Figure 9). In fact, we expected COX IV staining to be more abundant near the nucleus since mitochondria preferentially localize there. These preliminary studies suggest reduced mitochondrial density in MADD patient compared to controls, agreeing with the Western blot results for PGC-1α (Figure 8-C), a key regulator of mitochondrial biogenesis (88,89).

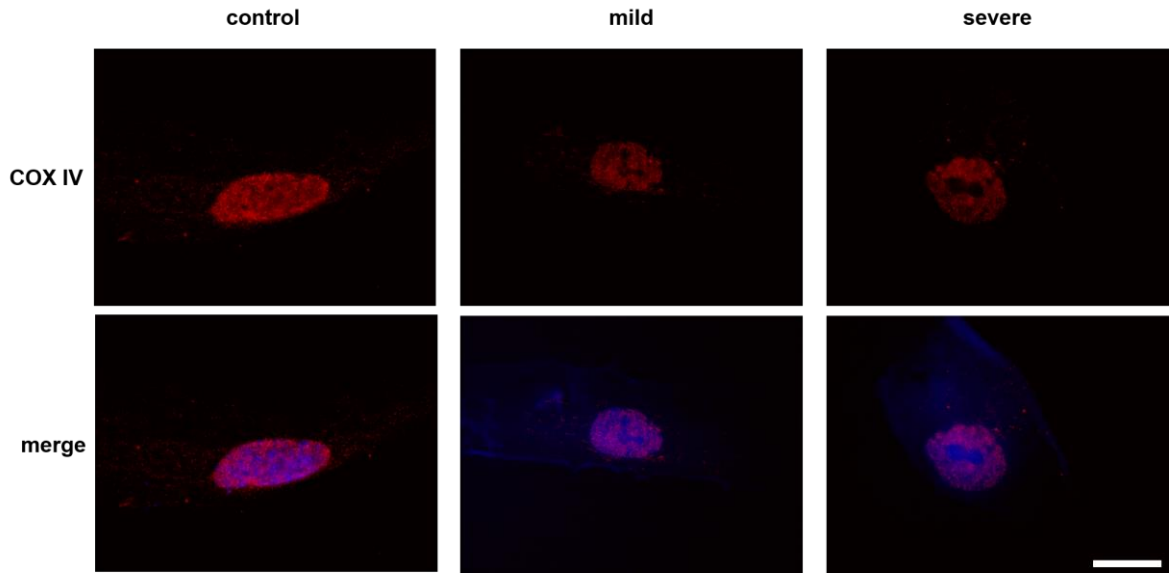

Figure 9. Effect of ETFDH deficiency on mitochondrial density in cultured skin fibroblasts from MADD patients. For control, mild and severe skin fibroblasts is presented a representative image of COX IV (red, Alexa Fluor® 594) and the merge between COX IV and the cell nuclei (blue, Hoechst 33258). Negative controls are presented in Appendix section. All images were obtained with a 100x magnification in an Olympus IX-81 inverted epifluorescence microscope. The scale bar of images is 20 μm.

4.5. Effect of MADD on apoptosis

In the present study we also evaluated the contribution of apoptotic pathways to MADD pathogenesis. Since our focus was on mitochondria, expression levels of proteins from the intrinsic pathway was measured, specifically bcl-2 associated X protein (Bax) and bcl-2 related protein A1 (Bcl-2A1). The expression levels of cleaved caspase-3 (Casp-3), which is the active form of the enzyme, were also measured by Western blotting. In figure 10 are presented the results obtained.

The expression levels of the pro-apoptotic protein Bax were not significantly different in MADD patients compared to controls despite an overall tendency to reduced levels (Figure 10-A). MADD4 patient showed significantly lower levels compared to controls ($p < 0.05$). No significant differences of Bcl-2A1 protein levels were found among MADD patients and controls (Figure 10-B). The ratio between these two proteins (Bax:Bcl-2A1) was

significantly lower in severe MADD patients compared to controls (Figure 10-C). No significant differences of the ratio between Bax and Bcl-2A1 were noticed for mild MADD patients. Curiously, the protein levels of Casp-3 were significantly higher only for MADD4 ($p < 0.0001$; Figure 10-D). The protein levels for the other subjects were not detectable by Western blot.

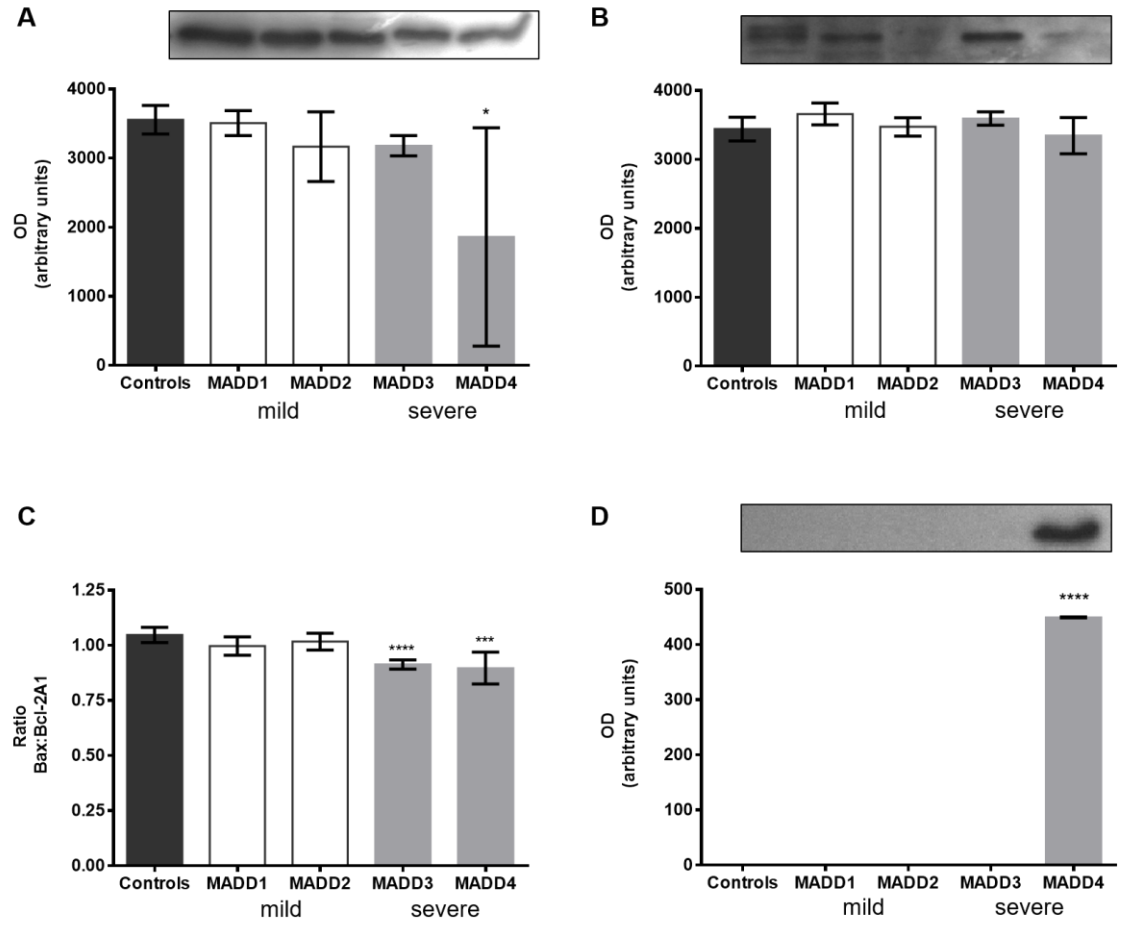

Figure 10. Effect of ETFDH deficiency on the content of Bax (**A**) and Bcl-2A1 (**B**), ratio between Bax and Bcl-2A1 (**C**) and Casp-3 (**D**) measured by Western Blotting in total homogenates of skin fibroblasts. MADD1 and MADD2 correspond to a mild form while MADD3 and MADD4 have severe form of MADD. Above each graph is presented a picture of the Western blots obtained. The values (mean ± SD) are expressed in arbitrary units of optical density (OD). * $p < 0.05$; *** $p < 0.001$; **** $p < 0.0001$.

5. Discussion

Multiple acyl-CoA dehydrogenase deficiency (MADD) is a rare disorder inherited in an autosomal recessive pattern which presents heterogeneous clinical phenotypes (29,30). Despite some degree of genotype-phenotype correlation, observed clinical spectrum suggests that other/specific molecular and cellular mechanisms may have a key role in MADD pathogenesis, in addition to mutations in *ETFA*, *ETFB* and *ETFDH* genes (26,33). Indeed, previous studies from our research group find that the mitochondrial proteome of patients with the same disease-causing genotype present different protein profiles. Moreover, patients with mild forms of MADD share some distinct protein signatures with severe forms and at the same time have distinctive expression patterns (unpublished data). These findings for MADD patients are consistent with those observed for LCHAD (unpublished data) and SCAD (110) deficiencies. In this way, our aim was to relate the regulation of biological processes associated to mitochondrial homeostasis with the severity of MADD, due to mutations on the gene that codifies the protein electron transfer flavoprotein dehydrogenase (ETFDH), evidencing similarities and differences. The integrated analysis of our data will help to better understand and characterize the molecular mechanisms underlying the mitochondrial dysfunction observed in these MADD patients.

To address the biological processes that regulate mitochondria homeostasis cultured skin fibroblasts from MADD patients were chosen. Cells isolated from other tissues as cardiac or skeletal muscles would be preferred since are more reliant on mitochondrial β-oxidation for energy purposes and fatty acids are preferential substrates (42,102,111,112). However, cultured skin fibroblasts are considered an attractive sample since skin biopsy is minimally invasive compared to other tissue biopsies and a large amount of cell material can be obtained (113,114). In fact, fibroblasts can be stored for long periods giving possibility of confirmatory posterior studies when new diagnostic tools become available. Moreover, this sample allows enzymatic measurements along with other biochemical and genetic analyzes (113). There have been reported several studies of mitochondrial proteome profiling in cultured fibroblasts for FAOD pathogenesis research (46,48,67,115,116).

In this way, cultured skin fibroblasts from four MADD patients, two with mild forms (MADD1 and MADD2) and two with severe forms (MADD3 and MADD4), were studied. MADD1 and MADD2 patients are both homozygous for the mutation p.R175H that introduces a substitution of arginine 175 with histidine in the FAD binding domain of

ETFDH (46). In opposite, MADD3 is homozygous for the mutation p.X618QextX14 which results in a protein extension of thirteen amino acids in C'-terminal of ETFDH due to a mutation in the stop codon that introduces another one that codifies glutamine (X618Q) and allows the continuous of translation until it reaches a different stop codon. MADD4 patient is compound heterozygous for p.X618QextX14 and p.E412X, which results in a truncated protein due to a mutation in the codon that codifies aspartate and introduces a premature stop codon (E412X). While the first two patients harbored a missense variation that impairs ETF/ETFDH complex functionality, the other two presented frameshift and nonsense mutations which lead to altered ETFDH protein that is most probably degraded/partially degraded by cell PQC system. Our results for the ETFDH expression levels detected by Western blotting corroborate these findings since MADD3 and MADD4 patients showed a significant decrease of the protein expression compared to controls, whereas MADD1 and MADD2 did not show significant decreased levels (Figure 5). Previous studies reported an absence of this protein in both severe and mild MADD forms (46,48). However, ETFDH absence in the study from Rocha *et al.* (48) was determined in isolated mitochondria, suggesting that this protein was not correctly transported to the mitochondria. Our results do not exclude the possibility of ETFDH absence in mitochondria in severe forms of MADD since we analyzed whole cell homogenates. Yotsumoto *et al.* (46) have also performed the analysis of ETFDH deficiency in whole cell homogenates, although the mild patients studied by them have a different genotype from ours and they probably used a different primary antibody targeting ETFDH protein. A more robust analysis of ETFDH protein in these patients may be considered, through measurement of enzyme activity because it correlates with functionality and there have been efforts to associate the enzyme activity with disease phenotypes (117).

In overall, we found that the ETFDH deficiency results in the down-regulation of mitochondrial biogenesis in MADD cultured skin fibroblasts evidenced by the significant decreased levels of peroxisome proliferator-activated receptor γ coactivator 1 alpha (PGC-1α) reported in all patients. Similarly, significant decreased levels of glyceraldehyde-3-phosphate dehydrogenase (GAPDH) in all MADD patients points to a metabolic adaptation in consequence of ETFDH deficiency. For the other biological processes

assessed we found differences among MADD patients. In fact, several proteins from these processes presented different expression levels among patients with the same genotype.

We hypothesized based on previous studies that ETFDH deficiency has impact on mitochondrial biogenesis and mitophagy, since these mechanisms are usually activated to counteract the disease-related mitochondrial dysfunction. Mitochondrial biogenesis was down-regulated, evaluated by significant decreased levels of PGC-1α in all MADD patients (Figure 8). To consolidate these results, immunocytochemistry studies were also performed in order to evaluate mitochondrial density. The preliminary qualitative data suggest decreased mitochondrial density (Figure 9), being in accordance with the down-regulation of PGC-1α. Different regulation mechanisms of this key regulator of mitochondrial biogenesis have been reported in several studies (102,118,119). Up-regulation of *PPAR* genes was reported in both MADD and riboflavin-responsive MADD (RR-MADD) patients, suggesting a compensatory mechanism of cells to counteract the damaged mitochondria inefficient in lipid metabolism (102,118), whereas a down-regulation of PGC-1α was also reported (119). On the other hand, mitophagy was found differently expressed in MADD patients. In fact, only patients with mild forms of MADD showed significant reduced levels of autophagy protein 5 (ATG5). This autophagic protein is essential for the autophagosome formation being considered a good mitophagy marker (52). Thus, the reduced levels of this protein in MADD1 and MADD2 suggest that mitophagy is down-regulated in these two mild MADD patients. However, this down-regulation of ATG5 did not seem to be correlated with an increased mitochondrial density considering the decreased PGC-1α levels in all patients. In accordance with these results, we found no alterations in citrate synthase (CS) activity for mild MADD patients. Thus, this corroborates with no increases in mitochondrial density since CS is considered as a good indicator of the number of mitochondria/mitochondrial mass on cells (108). However, severe MADD patients presented significant changes which require further analysis of these biochemical processes. In fact, MADD3 showed increased CS activity which may be explained by a compensatory mechanism with up-regulation of Krebs cycle, while MADD4 showed significantly higher levels of mitochondrial transcription factor A (mtTFA). Mitochondrial morphology and number should be evaluated in order to better understand the differences found among MADD patients in these processes. Mitotracker

assessment and markers of fusion/fission events may be considered to evaluate other signs of different phases of mitophagy. In fact, inhibition of fusion detected by decreased levels of mitofusin 2 (Mfn2), with increased mitophagy and fractionation were previously reported in RR-MADD patients (102).

PGC-1α is a key regulator of a huge variety of mitochondrial proteins (89). Indeed, down-regulation of PGC-1α have been associated with down-expression of several mitochondrial enzymes including FAO enzymes and sirtuin 3 (SIRT3) (119). Our findings evidenced a down-regulation of SIRT3 in MADD patients (Figure 7), being consistent with previous studies (67,119). SIRT3 is an essential mitochondrial regulator enzyme since it controls the activity of key metabolic and antioxidant enzymes by direct deacetylation and also indirectly by decreasing ROS-induced stability of hypoxia-inducible factor-1α (HIF-1α) (98,120). Thus, SIRT3 can act as a ROS suppressor due to its role on deacetylation and consequently activation of manganese superoxide dismutase (MnSOD) (121). No differences were noticed for the MnSOD levels, except for MADD3 who showed a significant decrease compared to controls. There are no straight results for MnSOD levels in literature for MADD patients. In fact, some studies reported down-regulation of MnSOD in RR-MADD patients (67,111), while other demonstrated an overexpression of this antioxidant enzyme for both mild and severe forms of MADD (48). Given the decreased levels of SIRT3 in almost all patients we were expecting similarly a down-regulation of MnSOD levels. However, the regulation of MnSOD by SIRT3 may not be sufficient to influence protein levels and thus enzymatic activity of MnSOD should be considered. Curiously, no significant differences on the content of carbonylated proteins were found in MADD patients, proving no differences in ROS production. We were expecting significantly higher levels of ROS and consequently of carbonylated proteins in MADD patients because it was previously described that MADD as other FAOD are associated with increased ROS production (8,67,118). The different results obtained for MnSOD and carbonylated proteins levels suggest that other assays should be performed to better characterize the oxidative status associated with ETFDH deficiency.

Previous studies have demonstrated a metabolic reprograming towards glycolysis with up-regulated genes and proteins of glycolysis and down-regulation of oxidative

phosphorylation (OXPHOS) in MADD and RR-MADD patients (48,67,118). We found significantly lower levels of GAPDH in all MADD patients (Figure 6). This protein plays an important role in glycolysis and gluconeogenesis (122). Our results for GAPDH were not consist with the previous mentioned (48,118). These studies were performed in isolated mitochondria, whereas we analyzed whole cell homogenates suggesting a possible explanation for the different results mentioned. In fact, overexpression of GAPDH in mitochondria has been associated with apoptotic events (123,124). Fibroblasts were cultured in medium containing glucose, pyruvate and large amounts of amino acids and vitamins, so we were expecting an increase in glycolytic enzymes. However, the overall down-regulation of GAPDH suggest a metabolic adaptation probably towards the use of other energetic substrates instead of glucose. In these way, search for other energetic metabolites and measurement of aminotransferases activity should be performed in cultured skin fibroblasts from MADD patients. In addition, analysis of cultured cells from other tissues such as muscle and liver may be of interest since these organs are the mainly affected in FAOD disorders (102,112,117). Indeed, this medium with glucose and no lipids is not the best option to test ETFDH deficiency. However, in a medium rich in fatty acids the proliferation of fibroblasts is impaired.

Significant reduced activity of ATP synthase was noticed for all patients with the exception of MADD2. The protein levels of ATP synthase α subunit (ATPase α) corroborated the enzymatic measurement, although without statistical significance. This down-regulation was consistent with previous results reported in the literature (48,111), thus suggesting that OXPHOS integrity is impaired with, consequently, reduced levels of produced ATP. No differences were noticed for the ratio between GAPDH and ATPase α in MADD patient, except for MADD3 who presented significant reduced values. In fact, the down-regulation of OXPHOS may be an initiator of the Warburg effect, which represents a shifting from OXPHOS to glycolysis for energy and biosynthetic intermediates production (125). Our results suggest a metabolic adaptation to compensate ATP deficiency at the mitochondria similar to those previous described but without increased levels of GADPH (8).

Regarding apoptosis, we found different protein expression patterns among MADD patients and controls (Figure 10). Significantly lower levels of the pro-apoptotic bcl-2

associated X protein (Bax) were noticed only for MADD4 patient. Similarly, no differences were found for the anti-apoptotic bcl-2 related protein A1 (Bcl-2A1) in MADD patients. Consequently, no significant differences of the ratio between Bax and Bcl-2A1 were noticed for mild MADD patients, although this ratio was significantly lower in severe MADD patients. In general, we can conclude that these results suggest that the intrinsic apoptotic pathway is not being activated or is down-regulated in MADD disease. This is not consistent with previous findings from our group (48) and other groups (67,112), which have reported overexpression of pro-apoptotic proteins including Smac/diablo, anexin and girdin. Curiously, MADD4 patient showed significantly higher levels of cleaved caspase-3 (Casp-3). This result clearly suggest an up-regulation of apoptosis, being in accordance with the results reported in the literature (48). Casp-3 may be activated by other caspases besides the intrinsic apoptotic activation (126,127). In fact, several studies have reported an activation of caspase-12 (Casp-12) that leads to activation of Casp-3 in response of endoplasmic reticulum (ER) stress-induced (127,128). However, it was also reported an interplay of bcl-2 family proteins such as Bax and Bak in the activation of Casp-12 and that this protein is expressed in small amounts in humans (129). These findings make us hypothesize that mitochondria-ER interactions may be modulated in MADD pathogenesis and thus ER dynamics studies should also be performed. In addition, the activity of Casp-3 as other caspases (Casp-8, Casp-9 and Casp-12) should be measured in order to better understand the contribution of apoptotic pathways to MADD pathogenesis. Furthermore, since autophagy proteins are also targets of executioner caspases including Casp-3 (130), the integrated study of both autophagic and apoptotic proteins may contribute to better elucidate the mitochondrial dysfunctionality associated with MADD.

In overall our study provides a global perspective of the mitochondrial dynamics in the two forms of MADD, mild and severe. Both forms presented down-regulation of mitochondrial biogenesis and metabolic adaptation. However, for the other biological processes assessed we did not find a pattern for the expressed proteins in MADD patients. Indeed, the different results obtained for the mechanisms studied may explain, at least in part, the variety of phenotypes observed in MADD patients. Despite the reduced number of patients due to the rarity of this disease, we can conclude that there is no straight full correlation

between disease severity and mitochondrial adaptations. Figure 11 represents an integrated perspective of the molecular mechanisms modulated by ETFDH deficiency in MADD patients.

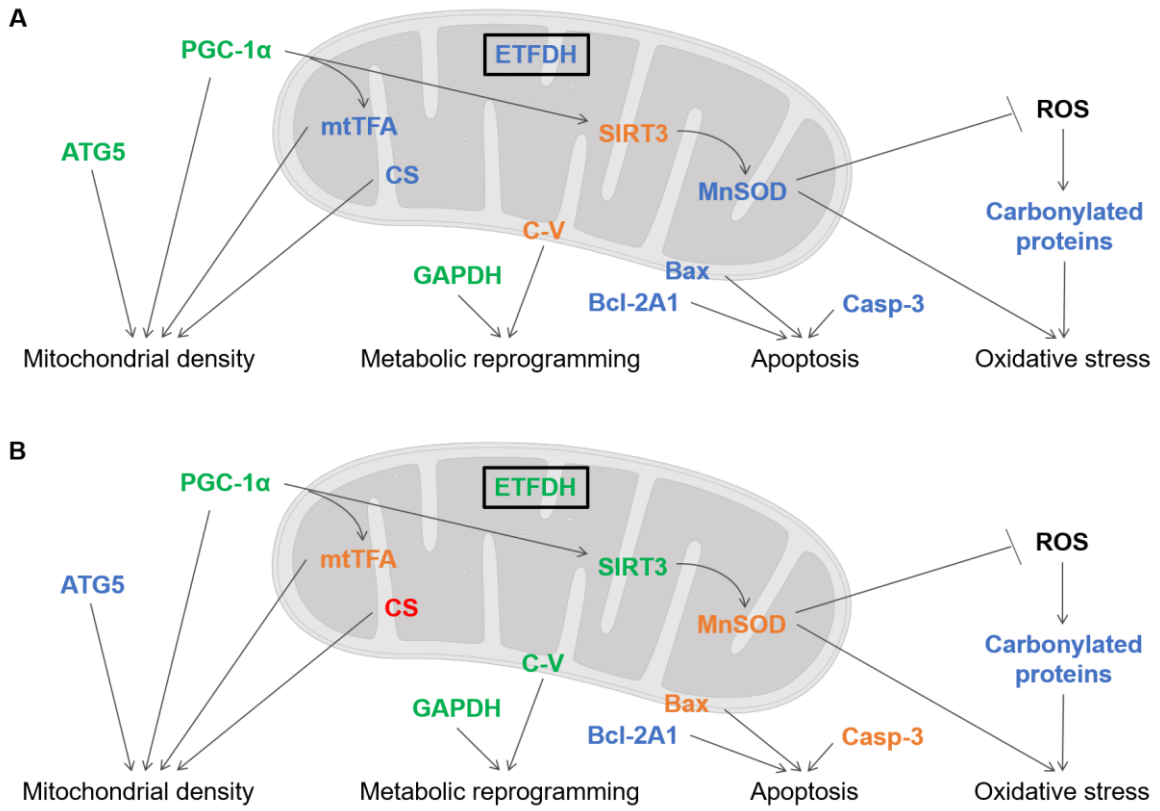

Figure 11. Integrated perspective of molecular mechanisms modulated by ETFDH deficiency in mild (**A**) and severe (**B**) forms of MADD. The proteins analyzed in the present study are highlighted with the up-regulated presented in red and the down-regulated in green. Proteins with no expression variation are presented in blue and proteins differently expressed between patients are presented in orange. These proteins belong to different pathways that relate to mitochondria and many of them are specifically expressed on mitochondrion and thus these results for the different patients may explain why MADD is such a heterogeneous disorder. Figure made with *Servier Medical Art*. Abbreviations: ATG5: autophagy protein 5, Bax: bcl-2 associated X protein, Bcl-2A1: bcl-2 related protein A1, Casp-3: cleaved caspase-3, CS: citrate synthase, C-V: ATP synthase, ETFDH: electron transfer flavoprotein dehydrogenase, GAPDH: glyceraldehyde-3-phosphate dehydrogenase, MnSOD: manganese superoxide dismutase, mtTFA: mitochondrial transcription factor A, PGC-1α: peroxisome proliferator-activated receptor γ coactivator 1 alpha, SIRT3: sirtuin 3, ROS: reactive oxygen species.

6. Conclusion and Future perspectives

The integrated analysis of data obtained from the analyzes of cultured fibroblasts from both mild and severe MADD patients, allowed us to conclude that there is no straight full correlation between disease severity and mitochondrial adaptations. Indeed, both forms of the disease presented down-regulation of mitochondrial biogenesis and metabolic adaptation highlighted by lower levels of PGC-1α and GAPDH, respectively, in all MADD patients. For other biological processes assessed we did not find a clear relation between the expressed proteins and MADD phenotype. Expression levels of SIRT3 and activity of ATP synthase were found decreased in almost all patients, suggesting a mitochondrial dysfunction due to down-regulation of SIRT3-mitochondrial targets and ATP production. Down-regulation of SIRT3 was corroborated by decreased levels of PGC-1α. The expression levels of the other proteins analyzed were more diverse among MADD patients. The divergent results obtained for the several pathways related to mitochondrial dynamics may explain, at least in part, the heterogeneous phenotypes associated with MADD pathogenesis.

MADD as other FAOD is a rare disorder of metabolism with high mortality rates. In this way, more studies are needed to better understand the genotype-phenotype correlation, involving other tissues that preferentially use FAO as energy source. For example, knock-down of ETFDH in cardiomyocytes or hepatocytes may be performed. Cell viability assays are also of high importance since they may justify such differences in patients with the same mutation. The analysis of the contribution of other energetic metabolites such as amino acids and pyruvate would be interestingly to better comprehend the metabolic adaptation related to ETFDH deficiency. In parallel, the study of other apoptotic proteins as well as other mitophagy and fusion/fission markers will certainly help to better understand the differences among the MADD patients. Similarly, the study of other stress-induced organelles including endoplasmic reticulum and its interplay with mitochondria would also contribute to explain the mitochondrial dysfunction.

7. References

1. Sahai I, Marsden D. Newborn screening. Crit Rev Clin Lab Sci. 2009;46(2):55–82.

2. Kompare M, Rizzo WB. Mitochondrial fatty-acid oxidation disorders. Semin Pediatr Neurol. 2008;15(3):140–9.

3. Lindner M, Hoffmann GF, Matern D. Newborn screening for disorders of fatty-acid oxidation: experience and recommendations from an expert meeting. J Inherit Metab Dis. 2010;33(5):521–6.

4. Rocha H, Castiñeiras D, Delgado C, Egea J, Yahyaoui R, González Y. Birth prevalence of fatty acid β-oxidation disorders in Iberia. JIMD Reports. 2014;16:89–94.

5. Wilcken B, Wiley V. Newborn screening. Pathology. 2008;40(2):104–15.

6. Wagner M, Tonoli D, Varesio E, Hopfgartner G. The use of mass spectrometry to analyze dried blood spots. Mass Spectrom Rev. 2016;35(3):361–438.

7. Vilarinho L, Pinho e Costa P, Diogo L. Programa Nacional de Diagnóstico Precoce: Relatório 2015. 2016 [cited 2017 Sep 28]; Available from: http://hdl.handle.net/10400.18/4073

8. Olsen RKJ, Cornelius N, Gregersen N. Genetic and cellular modifiers of oxidative stress: What can we learn from fatty acid oxidation defects? Mol Genet Metab. 2013;110:S31–9.

9. Houten SM, Wanders RJA. A general introduction to the biochemistry of mitochondrial fatty acid β-oxidation. J Inherit Metab Dis. 2010;33(5):469–77.

10. Wanders RJA, Ruiter JPN, IJlst L, Waterham HR, Houten SM. The enzymology of mitochondrial fatty acid beta-oxidation and its application to follow-up analysis of positive neonatal screening results. J Inherit Metab Dis. 2010;33(5):479–94.

11. Smeitink J, van den Heuvel L, DiMauro S. The genetics and pathology of oxidative phosphorylation. Nat Rev Genet. 2001;2(5):342–52.

12. Papa S, Martino PL, Capitanio G, Gaballo A, De Rasmo D, Signorile A. The oxidative phosphorylation system in mammalian mitochondria. In: Scatena R, Bottoni P, Giardina B, editors. Advances in Mitochondrial Medicine. Dordrecht: Springer Netherlands; 2012. p. 3–37.

13. Longo N, Frigeni M, Pasquali M. Carnitine transport and fatty acid oxidation. Biochim Biophys Acta BBA - Mol Cell Res. 2016;1863(10):2422–35.

14. Wanders RJ, Vreken P, den Boer ME, Wijburg FA, van Gennip AH, IJlst L. Disorders of mitochondrial fatty acyl-CoA β-oxidation. J Inherit Metab Dis. 1999;22(4):442–87.

15. Lazarow PB. Rat liver peroxisomes catalyze the β oxidation of fatty acids. J Biol Chem. 1978;253(5):1522–8.

16. Schrader M, Costello J, Godinho LF, Islinger M. Peroxisome-mitochondria interplay and disease. J Inherit Metab Dis. 2015;38(4):681–702.

17. Wanders RJA, Komen J, Kemp S. Fatty acid omega-oxidation as a rescue pathway for fatty acid oxidation disorders in humans. FEBS J. 2011;278(2):182–94.

18. Lund M, Olsen RK, Gregersen N. A short introduction to acyl-CoA dehydrogenases; deficiencies and novel treatment strategies. Expert Opin Orphan Drugs. 2015;3(12):1375–86.

19. Ensenauer R, He M, Willard J-M, Goetzman ES, Corydon TJ, Vandahl BB. Human acyl-CoA dehydrogenase-9 plays a novel role in the mitochondrial β-oxidation of unsaturated fatty acids. J Biol Chem. 2005;280(37):32309–16.

20. Toogood HS, Leys D, Scrutton NS. Dynamics driving function − new insights from electron transferring flavoproteins and partner complexes. FEBS J. 2007;274(21):5481–504.

21. Moczulski D, Majak I, Mamczur D. An overview of β-oxidation disorders. Postepy Hig Med Doswiadczalnej. 2009;63:266–77.

22. Vockley J, Whiteman DA. Defects of mitochondrial β-oxidation: a growing group of disorders. Neuromuscul Disord. 2002;12(3):235–46.

23. Sim KG, Hammond J, Wilcken B. Strategies for the diagnosis of mitochondrial fatty acid β-oxidation disorders. Clin Chim Acta. 2002;323(1):37–58.

24. Wilcken B. Fatty acid oxidation disorders: outcome and long-term prognosis. J Inherit Metab Dis. 2010;33(5):501–6.

25. Wajner M, Amaral AU. Mitochondrial dysfunction in fatty acid oxidation disorders: insights from human and animal studies. Biosci Rep. 2016;36(1):e00281–93.

26. Olsen RKJ, Andresen BS, Christensen E, Bross P, Skovby F, Gregersen N. Clear relationship between *ETF/ETFDH* genotype and phenotype in patients with multiple acyl-CoA dehydrogenation deficiency. Hum Mutat. 2003;22(1):12–23.

27. Olpin SE. Pathophysiology of fatty acid oxidation disorders and resultant phenotypic variability. J Inherit Metab Dis. 2013;36(4):645–58.

28. Gregersen N, Andresen BS, Corydon MJ, Corydon TJ, Olsen RKJ, Bolund L. Mutation analysis in mitochondrial fatty acid oxidation defects: exemplified by acyl-CoA dehydrogenase deficiencies, with special focus on genotype-phenotype relationship. Hum Mutat. 2001;18(3):169–89.

29. Frerman FE, Goodman SI. Deficiency of electron transfer flavoprotein or electron transfer flavoprotein: ubiquinone oxidoreductase in glutaric acidemia type II fibroblasts. Proc Natl Acad Sci USA. 1985;82(13):4517–20.

30. Frerman FE, Goodman SI. Defects of electron transfer flavoprotein and electron transfer flavoprotein-ubiquinone oxidoreductase: glutaric acidemia type II. In: Scriver CR, Beaudet AL, Sly WS, editors. The Metabolic and Molecular Bases of Inherited Disease. New York: McGraw-Hill; 2001. p. 2357–65.

31. Christensen E, Kølvraa S, Gregersen N. Glutaric aciduria type II: evidence for a defect related to the electron transfer flavoprotein or its dehydrogenase. Pediatr Res. 1984;18(7):663–7.

32. Abdenur JE, Chamoles NA, Schenone AB, Jorge L, Guinle A, Bernard C. Multiple acyl-CoA-dehydrogenase deficiency (MADD): use of acylcarnitines and fatty acids to monitor the response to dietary treatment. Pediatr Res. 2001;50(1):61–6.

33. Grünert SC. Clinical and genetical heterogeneity of late-onset multiple acyl-coenzyme A dehydrogenase deficiency. Orphanet J Rare Dis. 2014;9(1):117–24.

34. Przyrembel H, Wendel U, Becker K, Bremer HJ, Bruinvis L, Ketting D. Glutaric aciduria type II: report on a previously undescribed metabolic disorder. Clin Chim Acta Int J Clin Chem. 1976;66(2):227–39.

35. Goodman SI, Markey SP, Moe PG, Miles BS, Teng CC. Glutaric aciduria; a "new" disorder of amino acid metabolism. Biochem Med. 1975;12(1):12–21.

36. Hedlund GL, Longo N, Pasquali M. Glutaric acidemia type 1. Am J Med Genet C Semin Med Genet. 2006;142C(2):86–94.

37. Gregersen N, Andresen BS, Pedersen CB, Olsen RKJ, Corydon TJ, Bross P. Mitochondrial fatty acid oxidation defects—remaining challenges. J Inherit Metab Dis. 2008;31(5):643–57.

38. Bross P, Pedersen P, Winter V, Nyholm M, Johansen BN, Olsen RKJ. A polymorphic variant in the human electron transfer flavoprotein α-chain (α-T171) displays decreased thermal stability and is overrepresented in very-long-chain acyl-CoA dehydrogenase-deficient patients with mild childhood presentation. Mol Genet Metab. 1999;67(2):138–47.

39. Loehr JP, Goodman SI, Frerman FE. Glutaric acidemia type II: heterogeneity of clinical and biochemical phenotypes. Pediatr Res. 1990;27(3):311–5.

40. Gregersen N, Wintzensen H, Christensen SKE, Christensen MF, Brandt NJ, Rasmussen K. C6—C10-dicarboxylic aciduria: investigations of a patient with riboflavin responsive multiple acyl-CoA dehydrogenation defects. Pediatr Res. 1982;16(10):861–8.

41. Ho G, Yonezawa A, Masuda S, Inui K, Sim KG, Carpenter K. Maternal riboflavin deficiency, resulting in transient neonatal-onset glutaric aciduria type 2, is caused by a microdeletion in the riboflavin transporter gene *GPR172B*. Hum Mutat. 2011;32(1):E1976–84.

42. Olsen RKJ, Olpin SE, Andresen BS, Miedzybrodzka ZH, Pourfarzam M, Merinero B. *ETFDH* mutations as a major cause of riboflavin-responsive multiple acyl-CoA dehydrogenation deficiency. Brain. 2007;130(8):2045–54.

43. Cornelius N, Byron C, Hargreaves I, Fernandez Guerra P, Furdek AK, Land J. Secondary coenzyme Q10 deficiency and oxidative stress in cultured fibroblasts from patients with riboflavin responsive multiple acyl-CoA dehydrogenation deficiency. Hum Mol Genet. 2013;22(19):3819–27.

44. Olsen RKJ, Koňaříková E, Giancaspero TA, Mosegaard S, Boczonadi V, Mataković L. Riboflavin-responsive and -non-responsive mutations in FAD synthase cause multiple acyl-CoA dehydrogenase and combined respiratory-chain deficiency. Am J Hum Genet. 2016;98(6):1130–45.

45. Bosch AM, Stroek K, Abeling NG, Waterham HR, IJlst L, Wanders RJ. The Brown-Vialetto-Van Laere and Fazio Londe syndrome revisited: natural history, genetics, treatment and future perspectives. Orphanet J Rare Dis. 2012;7(1):83–9.

46. Yotsumoto Y, Hasegawa Y, Fukuda S, Kobayashi H, Endo M, Fukao T. Clinical and molecular investigations of Japanese cases of glutaric acidemia type 2. Mol Genet Metab. 2008;94(1):61–7.

47. Gregersen N, Olsen RKJ. Disease mechanisms and protein structures in fatty acid oxidation defects. J Inherit Metab Dis. 2010;33(5):547–53.

48. Rocha H, Ferreira R, Carvalho J, Vitorino R, Santa C, Lopes L. Characterization of mitochondrial proteome in a severe case of ETF-QO deficiency. J Proteomics. 2011;75(1):221–8.

49. Alves E, Henriques BJ, Rodrigues JV, Prudêncio P, Rocha H, Vilarinho L. Mutations at the flavin binding site of ETF:QO yield a MADD-like severe phenotype in *Drosophila*. Biochim Biophys Acta BBA - Mol Basis Dis. 2012;1822(8):1284–92.

50. Gregersen N, Hansen J, Palmfeldt J. Mitochondrial proteomics—a tool for the study of metabolic disorders. J Inherit Metab Dis. 2012;35(4):715–26.

51. Schuck PF, da Costa Ferreira G, Tonin AM, Viegas CM, Busanello ENB, Moura AP. Evidence that the major metabolites accumulating in medium-chain acyl-CoA dehydrogenase deficiency disturb mitochondrial energy homeostasis in rat brain. Brain Res. 2009;1296:117–26.

52. Ding W-X, Yin X-M. Mitophagy: mechanisms, pathophysiological roles, and analysis. Biol Chem. 2012;393(7):547–64.

53. Fischer F, Hamann A, Osiewacz HD. Mitochondrial quality control: an integrated network of pathways. Trends Biochem Sci. 2012;37(7):284–92.

54. Komen JC, Thorburn DR. Turn up the power - pharmacological activation of mitochondrial biogenesis in mouse models. Br J Pharmacol. 2014;171(8):1818–36.

55. Gianazza E, Eberini I, Sensi C, Barile M, Vergani L, Vanoni MA. Energy matters: mitochondrial proteomics for biomedicine. Proteomics. 2011;11(4):657–74.

56. Halliwell B, Cross CE. Oxygen-derived species: their relation to human disease and environmental stress. Environ Health Perspect. 1994;102(Suppl 10):5–12.

57. Pieczenik SR, Neustadt J. Mitochondrial dysfunction and molecular pathways of disease. Exp Mol Pathol. 2007;83(1):84–92.

58. Seifert EL, Estey C, Xuan JY, Harper M-E. Electron transport chain-dependent and -independent mechanisms of mitochondrial H_2O_2 emission during long-chain fatty acid oxidation. J Biol Chem. 2010;285(8):5748–58.

59. St-Pierre J. Topology of superoxide production from different sites in the mitochondrial electron transport chain. J Biol Chem. 2002;277(47):44784–90.

60. Circu ML, Aw TY. Reactive oxygen species, cellular redox systems, and apoptosis. Free Radic Biol Med. 2010;48(6):749–62.

61. Lluis JM, Buricchi F, Chiarugi P, Morales A, Fernandez-Checa JC. Dual role of mitochondrial reactive oxygen species in hypoxia signaling: activation of nuclear factor-κB via c-SRC–and oxidant-dependent cell death. Cancer Res. 2007;67(15):7368–77.

62. Schmidt SP, Corydon TJ, Pedersen CB, Vang S, Palmfeldt J, Stenbroen V. Toxic response caused by a misfolding variant of the mitochondrial protein short-chain acyl-CoA dehydrogenase. J Inherit Metab Dis. 2011;34(2):465–75.

63. Zhi X, Feng W, Rong Y, Liu R. Anatomy of autophagy: from the beginning to the end. Cell Mol Life Sci. 2017 (in press).

64. Lemasters JJ, Nieminen A-L, Qian T, Trost LC, Elmore SP, Nishimura Y. The mitochondrial permeability transition in cell death: a common mechanism in necrosis, apoptosis and autophagy. Biochim Biophys Acta BBA-Bioenerg. 1998;1366(1):177–96.

65. Elmore SP, Qian T, Grissom SF, Lemasters JJ. The mitochondrial permeability transition initiates autophagy in rat hepatocytes. FASEB J. 2001;15(12):2286–7.

66. Fortun J, Dunn WA, Joy S, Li J, Notterpek L. Emerging role for autophagy in the removal of aggresomes in Schwann cells. J Neurosci. 2003;23(33):10672–80.

67. Cornelius N, Corydon TJ, Gregersen N, Olsen RKJ. Cellular consequences of oxidative stress in riboflavin responsive multiple acyl-CoA dehydrogenation deficiency patient fibroblasts. Hum Mol Genet. 2014;23(16):4285–301.

68. Lyamzaev KG, Nepryakhina OK, Saprunova VB, Bakeeva LE, Pletjushkina OY, Chernyak BV. Novel mechanism of elimination of malfunctioning mitochondria (mitoptosis): formation of mitoptotic bodies and extrusion of mitochondrial material from the cell. Biochim Biophys Acta BBA - Bioenerg. 2008;1777(7–8):817–25.

69. Skulachev VP. Programmed death phenomena: from organelle to organism. Ann NY Acad Sci. 2002;959(1):214–37.

70. Arnoult D, Rismanchi N, Grodet A, Roberts RG, Seeburg DP, Estaquier J. Bax/Bak-dependent release of DDP/TIMM8a promotes Drp1-mediated mitochondrial fission and mitoptosis during programmed cell death. Curr Biol. 2005;15(23):2112–8.

71. Pop C, Salvesen GS. Human caspases: activation, specificity, and regulation. J Biol Chem. 2009;284(33):21777–81.

72. Elmore S. Apoptosis: a review of programmed cell death. Toxicol Pathol. 2007;35(4):495–516.

73. Jiang X, Wang X. Cytochrome *C*-mediated apoptosis. Annu Rev Biochem. 2004;73(1):87–106.

74. Chen Q, Lesnefsky EJ. Depletion of cardiolipin and cytochrome *c* during ischemia increases hydrogen peroxide production from the electron transport chain. Free Radic Biol Med. 2006;40(6):976–82.

75. Lorenzo HK, Susin SA. Therapeutic potential of AIF-mediated caspase-independent programmed cell death. Drug Resist Updat. 2007;10(6):235–55.

76. Susin SA, Lorenzo HK, Zamzami N, Marzo I, Snow BE, Brothers GM. Molecular characterization of mitochondrial apoptosis-inducing factor. Nature. 1999;397(6718):441–6.

77. Chan DC. Mitochondrial fusion and fission in mammals. Annu Rev Cell Dev Biol. 2006;22(1):79–99.

78. Hales KG, Fuller MT. Developmentally regulated mitochondrial fusion mediated by a conserved, novel, predicted GTPase. Cell. 1997;90(1):121–9.

79. Rojo M, Legros F, Chateau D, Lombès A. Membrane topology and mitochondrial targeting of mitofusins, ubiquitous mammalian homologs of the transmembrane GTPase Fzo. J Cell Sci. 2002;115(8):1663–74.

80. Chen H, Detmer SA, Ewald AJ, Griffin EE, Fraser SE, Chan DC. Mitofusins Mfn1 and Mfn2 coordinately regulate mitochondrial fusion and are essential for embryonic development. J Cell Biol. 2003;160(2):189–200.

81. Chen H, Chomyn A, Chan DC. Disruption of fusion results in mitochondrial heterogeneity and dysfunction. J Biol Chem. 2005;280(28):26185–92.

82. Cipolat S, de Brito OM, Dal Zilio B, Scorrano L. OPA1 requires mitofusin 1 to promote mitochondrial fusion. Proc Natl Acad Sci USA. 2004;101(45):15927–32.

83. Smirnova E, Griparic L, Shurland D-L, Van Der Bliek AM. Dynamin-related protein Drp1 is required for mitochondrial division in mammalian cells. Mol Biol Cell. 2001;12(8):2245–56.

84. Lee Y, Jeong S-Y, Karbowski M, Smith CL, Youle RJ. Roles of the mammalian mitochondrial fission and fusion mediators Fis1, Drp1, and Opa1 in apoptosis. Mol Biol Cell. 2004;15(11):5001–11.

85. Karbowski M, Jeong S-Y, Youle RJ. Endophilin B1 is required for the maintenance of mitochondrial morphology. J Cell Biol. 2004;166(7):1027–39.

86. Tondera D, Czauderna F, Paulick K, Schwarzer R, Kaufmann J, Santel A. The mitochondrial protein MTP18 contributes to mitochondrial fission in mammalian cells. J Cell Sci. 2005;118(14):3049–59.

87. Schmidt SP, Corydon TJ, Pedersen CB, Bross P, Gregersen N. Misfolding of short-chain acyl-CoA dehydrogenase leads to mitochondrial fission and oxidative stress. Mol Genet Metab. 2010;100(2):155–62.

88. Puigserver P, Wu Z, Park CW, Graves R, Wright M, Spiegelman BM. A cold-inducible coactivator of nuclear receptors linked to adaptive thermogenesis. Cell. 1998;92(6):829–39.

89. Jornayvaz FR, Shulman GI. Regulation of mitochondrial biogenesis. Essays Biochem. 2010;47:69–84.

90. Lin J, Wu H, Tarr PT, Zhang C-Y, Wu Z, Boss O. Transcriptional co-activator PGC-1α drives the formation of slow-twitch muscle fibres. Nature. 2002;418(6899):797–801.

91. Wu Z, Puigserver P, Andersson U, Zhang C, Adelmant G, Mootha V. Mechanisms controlling mitochondrial biogenesis and respiration through the thermogenic coactivator PGC-1α. Cell. 1999;98(1):115–24.

92. St-Pierre J, Lin J, Krauss S, Tarr PT, Yang R, Newgard CB. Bioenergetic analysis of peroxisome proliferator-activated receptor coactivators 1α and 1β (PGC-1α and PGC-1β) in muscle cells. J Biol Chem. 2003;278(29):26597–603.

93. Higashida K, Kim SH, Jung SR, Asaka M, Holloszy JO, Han D-H. Effects of resveratrol and SIRT1 on PGC-1α activity and mitochondrial biogenesis: a reevaluation. PLoS Biol. 2013;11(7):e1001603-14.

94. Wan Z, Root-Mccaig J, Castellani L, Kemp BE, Steinberg GR, Wright DC. Evidence for the role of AMPK in regulating PGC-1 alpha expression and mitochondrial proteins in mouse epididymal adipose tissue. Obesity. 2014;22(3):730–8.

95. Lim J-H, Gerhart-Hines Z, Dominy JE, Lee Y, Kim S, Tabata M. Oleic acid stimulates complete oxidation of fatty acids through protein kinase A-dependent activation of SIRT1-PGC1α complex. J Biol Chem. 2013;288(10):7117–26.

96. Akimoto T, Pohnert SC, Li P, Zhang M, Gumbs C, Rosenburg PB. Exercise stimulates *Pgc-1α* transcription in skeletal muscle through activation of the p38 MAPK pathway. J Biol Chem. 2005;280(20):19587–93.

97. Cantó C, Houtkooper RH, Pirinen E, Youn DY, Oosterveer MH, Cen Y. The NAD^+ precursor nicotinamide riboside enhances oxidative metabolism and protects against high-fat diet-induced obesity. Cell Metab. 2012;15(6):838–47.

98. Hirschey MD, Shimazu T, Goetzman E, Jing E, Schwer B, Lombard DB. SIRT3 regulates mitochondrial fatty-acid oxidation via reversible enzyme deacetylation. Nature. 2010;464(7285):121–5.

99. Schwer B, North BJ, Frye RA, Ott M, Verdin E. The human silent information regulator (Sir)2 homologue hSIRT3 is a mitochondrial nicotinamide adenine dinucleotide–dependent deacetylase. J Cell Biol. 2002;158(4):647–57.

100. Feige JN, Lagouge M, Canto C, Strehle A, Houten SM, Milne JC. Specific SIRT1 activation mimics low energy levels and protects against diet-induced metabolic disorders by enhancing fat oxidation. Cell Metab. 2008;8(5):347–58.

101. Lagouge M, Argmann C, Gerhart-Hines Z, Meziane H, Lerin C, Daussin F. Resveratrol improves mitochondrial function and protects against metabolic disease by activating SIRT1 and PGC-1α. Cell. 2006;127(6):1109–22.

102. Wen B, Li D, Shan J, Liu S, Li W, Zhao Y. Increased muscle coenzyme Q10 in riboflavin responsive MADD with *ETFDH* gene mutations due to secondary mitochondrial proliferation. Mol Genet Metab. 2013;109(2):154–60.

103. Lowry OH, Rosebrough NJ, Farr AL, Randall RJ. Protein measurement with the Folin phenol reagent. J Biol Chem. 1951;193(1):265–75.

104. Laemmli UK. Cleavage of structural proteins during the assembly of the head of bacteriophage T4. Nature. 1970;227(5259):680–5.

105. Robinson CE, Keshavarzian A, Pasco DS, Frommel TO, Winship DH, Holmes EW. Determination of protein carbonyl groups by immunoblotting. Anal Biochem. 1999;266(1):48–57.

106. Simon N, Papa K, Vidal J, Boulamery A, Bruguerolle B. Circadian rhythms of oxidative phosphorylation: effects of rotenone and melatonin on isolated rat brain mitochondria. Chronobiol Int. 2003;20(3):451–61.

107. Coore HG, Denton RM, Martin BR, Randle PJ. Regulation of adipose tissue pyruvate dehydrogenase by insulin and other hormones. Biochem J. 1971;125(1):115–27.

108. Idell-Wenger JA, Grotyohann LW, Neely JR. Coenzyme A and carnitine distribution in normal and ischemic hearts. J Biol Chem. 1978;253(12):4310–8.

109. Li Y, Park J-S, Deng J-H, Bai Y. Cytochrome c oxidase subunit IV is essential for assembly and respiratory function of the enzyme complex. J Bioenerg Biomembr. 2006;38(5):283–91.

110. Edhager AV, Stenbroen V, Nielsen NS, Bross P, Olsen RKJ, Gregersen N. Proteomic investigation of cultivated fibroblasts from patients with mitochondrial short-chain acyl-CoA dehydrogenase deficiency. Mol Genet Metab. 2014;111(3):360–8.

111. Gianazza E, Vergani L, Wait R, Brizio C, Brambilla D, Begum S. Coordinated and reversible reduction of enzymes involved in terminal oxidative metabolism in skeletal muscle mitochondria from a riboflavin-responsive, multiple acyl-CoA dehydrogenase deficiency patient. Electrophoresis. 2006;27(5–6):1182–98.

112. Wang W, Mohsen A-W, Uechi G, Schreiber E, Balasubramani M, Day B. Complex changes in the liver mitochondrial proteome of short chain acyl-CoA dehydrogenase deficient mice. Mol Genet Metab. 2014;112(1):30–9.

113. Rodenburg RJT. Biochemical diagnosis of mitochondrial disorders. J Inherit Metab Dis. 2011;34(2):283–92.

114. De Paepe B, Smet J, Vanlander A, Seneca S, Lissens W, De Meirleir L. Fluorescence imaging of mitochondria in cultured skin fibroblasts: a useful method for the detection of oxidative phosphorylation defects. Pediatr Res. 2012;72(3):232–40.

115. Palmfeldt J, Vang S, Stenbroen V, Pedersen CB, Christensen JH, Bross P. Mitochondrial proteomics on human fibroblasts for identification of metabolic imbalance and cellular stress. Proteome Sci. 2009;7(1):20-9.

116. Ferreira R, Rocha H, Almeida V, Padrão AI, Santa C, Vilarinho L. Mitochondria proteome profiling: a comparative analysis between gel- and gel-free approaches. Talanta. 2013;115:277–83.

117. Spiekerkoetter U. Mitochondrial fatty acid oxidation disorders: clinical presentation of long-chain fatty acid oxidation defects before and after newborn screening. J Inherit Metab Dis. 2010;33(5):527–32.

118. Song Y, Selak MA, Watson CT, Coutts C, Scherer PC, Panzer JA. Mechanisms underlying metabolic and neural defects in zebrafish and human multiple acyl-CoA dehydrogenase deficiency (MADD). Riley B, editor. PLoS ONE. 2009;4(12):e8329-40.

119. Olsen RKJ, Cornelius N, Gregersen N. Redox signalling and mitochondrial stress responses; lessons from inborn errors of metabolism. J Inherit Metab Dis. 2015;38(4):703–19.

120. Bell EL, Emerling BM, Ricoult SJH, Guarente L. SirT3 suppresses hypoxia inducible factor 1α and tumor growth by inhibiting mitochondrial ROS production. Oncogene. 2011;30(26):2986–96.

121. Tao R, Coleman MC, Pennington JD, Ozden O, Park S-H, Jiang H. Sirt3-mediated deacetylation of evolutionarily conserved lysine 122 regulates MnSOD activity in response to stress. Mol Cell. 2010;40(6):893–904.

122. Bruns G, Gerald P. Human glyceraldehyde-3-phosphate dehydrogenase in man-rodent somatic cell hybrids. Science. 1976;192(4234):54–6.

123. Huang J, Hao L, Xiong N, Cao X, Liang Z, Sun S. Involvement of glyceraldehyde-3-phosphate dehydrogenase in rotenone-induced cell apoptosis: relevance to protein misfolding and aggregation. Brain Res. 2009;1279:1–8.

124. Tarze A, Deniaud A, Le Bras M, Maillier E, Mollé D, Larochette N. GAPDH, a novel regulator of the pro-apoptotic mitochondrial membrane permeabilization. Oncogene. 2007;26(18):2606–20.

125. Maldonado EN, Lemasters JJ. Warburg revisited: regulation of mitochondrial metabolism by voltage-dependent anion channels in cancer cells. J Pharmacol Exp Ther. 2012;342(3):637–41.

126. Hu S, Snipas SJ, Vincenz C, Salvesen G, Dixit VM. Caspase-14 is a novel developmentally regulated protease. J Biol Chem. 1998;273(45):29648–53.

127. Nakagawa T, Zhu H, Morishima N, Li E, Xu J, Yankner BA. Caspase-12 mediates endoplasmic-reticulum-specific apoptosis and cytotoxicity by amyloid-β. Nature. 2000;403(6765):98–103.

128. Tan Y, Dourdin N, Wu C, De Veyra T, Elce JS, Greer PA. Ubiquitous calpains promote caspase-12 and JNK activation during endoplasmic reticulum stress-induced apoptosis. J Biol Chem. 2006;281(23):16016–24.

129. Heath-Engel HM, Chang NC, Shore GC. The endoplasmic reticulum in apoptosis and autophagy: role of the BCL-2 protein family. Oncogene. 2008;27(50):6419–33.

130. Wu H, Che X, Zheng Q, Wu A, Pan K, Shao A. Caspases: a molecular switch node in the crosstalk between autophagy and apoptosis. Int J Biol Sci. 2014;10(9):1072–83.

8. Appendix

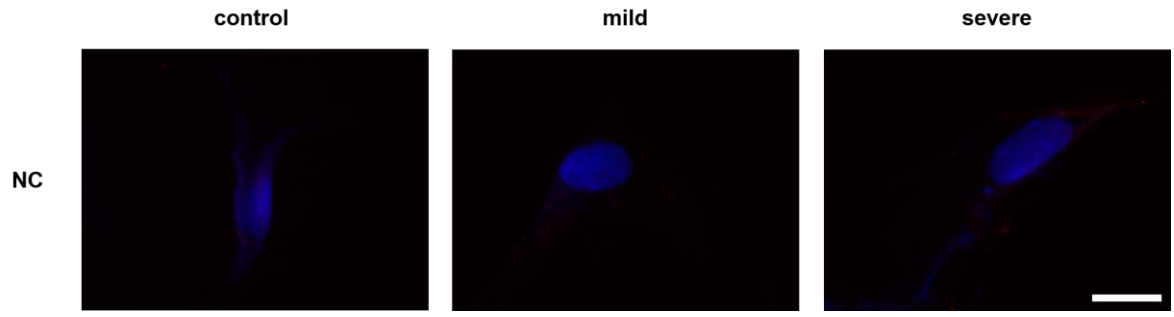

Figure 12. Effect of ETFDH deficiency on mitochondrial density in cultured skin fibroblasts from MADD patients. Negative control (NC) for control, mild and severe skin fibroblasts were obtained from incubation with blocking solution instead of primary antibody (rabbit polyclonal anti-COX IV). Representative image of the merge between COX IV (red, Alexa Fluor® 594) and the cell nuclei (blue, Hoechst 33258) for NC. The absence of red (COX IV) dots compared to the merge where the primary antibody was added (Figure 9), indicates that there is specificity for the primary antibody chosen. All images were obtained with a 100x magnification in an Olympus IX-81 inverted epifluorescence microscope. The scale bar of images is 20 μm.